Molecular Phylogenetics and Evolution 189 (2023) 107928

Contents lists available at ScienceDirect

Molecular Phylogenetics and Evolution

journal homepage: www.elsevier.com/locate/ympev

Impact of the climatic changes in the Pliocene-Pleistocene transition on Irano-Turanian species. The radiation of genus *Jurinea* (Compositae)

Sonia Herrando-Moraira [a], Cristina Roquet [b,*], The Cardueae Radiations Group (in alphabetical order):

[a] *Botanic Institute of Barcelona (IBB, CSIC-Ajuntament de Barcelona), Pg. del Migdia, s.n., 08038 Barcelona, Spain*
[b] *Systematics and Evolution of Vascular Plants (UAB) – Associated Unit to CSIC, Departament de Biologia Animal, Biologia Vegetal i Ecologia, Facultat de Biociències, Universitat Autònoma de Barcelona, 08193 Bellaterra, Spain*

ARTICLE INFO

Keywords:
Asteraceae
Biogeography
Diversification
Hyb-seq
Irano-Turanian region
Phylogeny

ABSTRACT

The Irano-Turanian region is one of the world's richest floristic regions and the centre of diversity for numerous xerophytic plant lineages. However, we still have limited knowledge on the timing of evolution and biogeographic history of its flora, and potential drivers of diversification remain underexplored. To fill this knowledge gap, we focus on the Eurasian genus *Jurinea* (ca. 200 species), one of the largest plant radiations that diversified in the region. We applied a macroevolutionary integrative approach to explicitly test diversification hypotheses and investigate the relative roles of geography vs. ecology and niche conservatism vs. niche lability in speciation processes. To do so, we gathered a sample comprising 77% of total genus richness and obtained data about (1) its phylogenetic history, recovering 502 nuclear loci sequences; (2) growth forms; (3) ecological niche, compiling data of 21 variables for more than 2500 occurrences; and (4) paleoclimatic conditions, to estimate climatic stability. Our results revealed that climate was a key factor in the evolutionary dynamics of *Jurinea*. The main diversification and biogeographic events that occurred during past climate changes, which led to colder and drier conditions, are the following: (1) the origin of the genus (10.7 Ma); (2) long-distance dispersals from the Iranian Plateau to adjacent regions (~7–4 Ma); and (3) the diversification shift during Pliocene-Pleistocene Transition (ca. 3 Ma), when net diversification rate almost doubled. Our results supported the pre-adaptation hypothesis, i.e., the evolutionary success of *Jurinea* was linked to the retention of the ancestral niche adapted to aridity. Interestingly, the paleoclimatic analyses revealed that in the Iranian Plateau long-term climatic stability favoured old-lineage persistence, resulting in current high species richness of semi-arid and cold adapted clades; whereas moderate climate oscillations stimulated allopatric diversification in the lineages distributed in the Circumboreal region. In contrast, growth form lability and high niche disparity among closely related species in the Central Asian clade suggest adaptive radiation to mountain habitats. In sum, the radiation of *Jurinea* is the result of both adaptive and non-adaptive processes influenced by climatic, orogenic and ecological factors.

1. Introduction

The study of evolutionary radiations is a hot topic in plant science research (Hughes et al., 2015), with the number of published articles on plant radiations increasing dramatically since 2000s (Stroud and Losos, 2016). Most studies to date have focused on lineages with outstanding species richness in plant diversity hotspots such as the Cape Floristic Region, the Mediterranean Basin, oceanic islands and archipelagos such as Macaronesia, or mountain ranges such as the Andes or the Himalayas (Hughes and Atchison, 2015). This type of research has allowed investigators to identify the main evolutionary and environmental factors shaping biodiversity patterns in these hotspots and assess their relative contributions. However, there are still species-rich regions where continental radiations have taken place that remain understudied from an evolutionary and biogeographic perspective. One of such knowledge gaps concerns the Irano-Turanian floristic region (hereafter IT; Takhtajan, 1986), whose biodiversity origins and biogeographic relationships with other regions remain poorly studied despite its relevance in terms

* Corresponding author at: Systematics and Evolution of Vascular Plants (UAB) – Associated Unit to CSIC, Departament de Biologia Animal, Biologia Vegetal i Ecologia, Facultat de Biociències, Universitat Autònoma de Barcelona, 08193 Bellaterra, Spain.
E-mail address: cristina.roquet@uab.cat (C. Roquet).

https://doi.org/10.1016/j.ympev.2023.107928
Received 30 March 2023; Received in revised form 7 September 2023; Accepted 12 September 2023
Available online 14 September 2023

of plant diversity (32,000 species; Takhtajan, 1986; Sales and Hedge, 2013) and endemism (25–40%; Zohary, 1981; Takhtajan, 1986). Indeed, this region harbours two global biodiversity hotspots: the Irano-Anatolian region and the Mountains of Central Asia (Mittermeier et al., 2011).

The IT region is located in Western-Central Asia, surrounded by the Circumboreal floristic region in the north, the eastern Mediterranean in the west, Arabia in the south, and East Asia in the east (see Manafzadeh et al., 2017 for a review of its circumscription). One of most remarkable characteristics of IT is its continental climate, with cold winters, warm-dry summers, and a high precipitation seasonality (Djamali et al., 2012). Topographically, IT presents high landscape heterogeneity and wide altitudinal gradients, with large mountains ranges (Taurus, Zagros, Alborz, Kopet-Dagh, Pamir, Tian Shan, Western Himalayas) and broad plateaus (Anatolian, Iranian, and Qinghai-Tibetan plateaus). The geo-climatic configuration of IT has likely favoured the diversification of xerophytes, which are adapted to arid or semi-arid environments under low water availability conditions, such as steppe elements (e.g., mega-diverse genera like *Acantholimon*, *Acanthophyllum*, *Astragalus*, *Cousinia*, *Eremostachys* and *Eremurus*; Manafzadeh et al., 2017) or C4 metabolism plants (e.g. *Eragrostis, Stipagrostis*; Rudov et al., 2020). Diversification is especially noticeable in mountain habitats: for instance, endemic richness of Compositae in Iran reaches maximum values at mid-elevations in mountain ranges (1400–2100 m a.s.l.; Noroozi et al., 2019).

However, limited information is available about the origins and drivers of diversification of the IT flora (see a synthesis in Manafzadeh et al., 2017). Regarding the timing of the origin of IT elements, several hypotheses have been proposed. The oldest scenario points to a Cretaceous origin (145–66 Ma; Takhtajan, 1986). Other studies suggest the early Eocene as a period of initial divergence of lineages (55 Ma; Manafzadeh et al., 2014), or during the drying of the Tethys Sea in the Neogene (34 Ma; Zohary, 1973). Nevertheless, recent time-calibrated phylogenies of diverse groups suggest that IT elements originated much more recently, from the Miocene onwards (Wu et al., 2015; Lauterbach et al., 2019), with special emphasis on the Pliocene-Pleistocene (Moharrek et al., 2019; Mahmoudi Shamsabad et al., 2021). Regarding potential drivers of diversification, the orogenic activity during the Miocene deeply shaped the IT landscape (Manafzadeh et al., 2017) and likely impacted the evolution of its flora: the second collision of the Afro-Arabian plate against the Eurasian plate originated the uplift of the Iranian Plateau ca. 13 Ma, and subsequent uplift and deformations occurred from 15 to 5 Ma along the Zagros, Alborz, Kopeth Dagh, and Caucasus mountains (Mouthereau, 2011). Such orogenic activity may have been an important driver of species diversification increasing habitat heterogeneity and thus ecological opportunities and favouring allopatric speciation through vicariance. On the other hand, the distribution and diversity of organisms have also likely been impacted by past climatic changes such as: (1) the aridification of central Asia during mid-late Miocene (17–5 Ma; Miao et al., 2012); (2) the global climate cooling between ~3.2–2.7 Ma, a period known as the Pliocene-Pleistocene transition (PPT; Lisiecki and Raymo, 2005); and (3) the drastic climatic oscillations during the Quaternary glacial-interglacial cycles (Zachos et al., 2001).

Recent methodological advances in comparative phylogenetic analyses (Borges et al., 2019), biogeographic history inference (Matzke, 2013), and models of diversification (e.g. Etienne et al., 2012; Morlon et al., 2016), together with ecological niche modelling and high-resolution paleoclimatic datasets (*PaleoClim*; Brown et al., 2018), make it now possible to investigate the relative importance of abiotic and biotic factors on the diversification of IT taxa, and allow testing hypotheses about macroevolutionary and biogeographic dynamics of the IT flora proposed by previous authors (reviewed in Manafzadeh et al., 2017). Two main scenarios, not mutually exclusive, may explain IT diversification: (1) vicariance through uplifts of mountain ranges (geographic speciation); and (2) ecological speciation. In the first scenario, species diverged by allopatry driven by geologic or climatic processes, and the ecological niche has been preserved among sister taxa (niche conservatism; Wiens et al., 2010). In the second, lineages diverged by adaptation to new ecological zones (niche divergence). Concerning the biogeographic interactions of IT with other regions, previous studies have suggested that IT constituted an important source of taxa to adjacent regions, especially contributing to the assemblage of the Mediterranean flora (Jabbour and Renner, 2011; Salvo et al., 2011; Manafzadeh et al., 2014; Lauterbach et al., 2019; Moharrek et al., 2019; Peterson et al., 2019; Mahmoudi Shamsabad et al., 2021). Two main hypotheses have been proposed regarding the temporal framework of dispersals from IT to the Mediterranean region: (1) during the early to late Miocene (Zohary, 1973; Manafzadeh et al., 2014); and (2) during Late Quaternary (Magyari et al., 2008). On the other hand, it is unknown whether IT also constituted an important source of xerophytic lineages for other hotspots of the rest of Eurasia.

Integrative studies on mega-genera based on well-resolved phylogenies are needed to significantly advance in our understanding of the relative roles of geological, climatic, biogeographic and ecological factors in the diversification of the IT flora (Manafzadeh et al., 2017). Here, we studied one of the largest plant radiations of the IT: the genus *Jurinea* Cass. (tribe Cardueae, Compositae), which includes ca. 200 species, of which ca. 70% occur in the IT (Susanna and Garcia-Jacas, 2007). *Jurinea* spans throughout Eurasia from latitude 20°N to 60°N, and from longitude 10°W to 120°E, and it is found in species-rich areas of the IT, especially in Iran, Afghanistan, and Central Asia Mountains (Rechinger and Wagenitz, 1979; Szukala et al., 2019). The genus is also present along the Mediterranean Basin, central-eastern Europe, European Russia, Himalayas, and East Asia. The predominant altitudinal range is around 1000–2000 m, although some species grow near the sea-level (like *J. kilaea* Azn.; Danin and Davis, 1975) and others up to the alpine belt (4500 m like *J. gilesii* (Hemsl.) N.Garcia, Herrando & Susanna; Rechinger and Wagenitz, 1979). Ecologically, *Jurinea* species mainly grow on mountain and rocky slopes, grasslands, steppes, pine-forest stands, forest margins, lake and riverbanks, and subalpine-alpine meadows (Iljin, 1962; Danin and Davis, 1975; Rechinger and Wagenitz, 1979). Several growth forms are found within the genus, each associated to particular habitats and reflecting different ecological strategies: (1) the only annual species, *J. modesta* Boiss., shows a peculiar growth form intermediate between the acaulescent rosette and the scapose form, and is adapted to the extreme arid habitat found in the foothills of the mountains of Afghanistan; (2) biennial plants characterized by long-foliose stems with soft and wide leaves (very different from the usually narrow, scariose or leathery leaves of all other *Jurinea* species) are found in humid valleys south of the Himalayas; (3) rosetted acaulescent perennials are always mountain-adapted plants; (4) scapose rosetted perennials usually represent an adaptation to Mediterranean climate or steppe with summer drought; and (5) foliose subshrubs are mostly adapted to semideserts.

The complex taxonomy of *Jurinea* has contributed to its understudied status. Historically, up to nine satellite genera have been recognized within it, though a recent phylogeny of subtribe Saussureinae based on Hyb-Seq data has shown that all of them are more properly accommodated as part of the large genus *Jurinea* (Herrando-Moraira et al., 2020, which included ca. 40 *Jurinea* spp.). The most complete phylogeny of *Jurinea* published to date includes only 81 spp., which represents one third of the genus diversity (Szukala et al., 2019). Although it provides a substantial contribution on the phylogenetic relationships, it is still notably incomplete in terms of taxonomic and biogeographic sampling, as it lacks many representatives from Central Asia, and it does not include a diversification analysis with explicit temporal and spatial frameworks. Therefore, the evolutionary history of the group is still to be unraveled.

In sum, our study aims to decipher the diversification history of *Jurinea* with the central goal to fill the knowledge gap concerning the evolution of the IT flora, investigating the three classical key issues addressed in radiation studies: tempo, mode, and diversification drivers.

We did so by integrating phylogenetic data with biogeographic history inference, diversification modelling, ancestral state reconstruction, and ecological niche modelling. Specifically, we first obtained a highly resolved time-calibrated tree based on high throughput molecular methods yielding 502 family-specific loci and including a wide taxon sampling (77%). Then, we conducted an analysis of biogeographic history inference to elucidate the relative contributions of *in situ* speciation versus vicariance to the IT flora, and to explore the potential impact of range expansions and contractions in the diversification dynamics of *Jurinea*. Next, we explicitly tested whether species diversification varied with time, climate or species-diversity; and whether the major climatic shifts that occurred during the PPT significantly impacted diversification dynamics. Furthermore, we investigated the relative importance of niche conservatism vs. niche divergence in speciation by measuring the phylogenetic signal of the environmental niche and growth form lability (i.e. the propensity of lineages to change growth form). Last, we identified stable climatic areas since the Pliocene to the present to assess how regional climatic fluctuations may have impacted *Jurinea*.

2. Materials and methods

Methods are described in greater detail with full references in the Supplementary Information.

2.1. Sampling strategy

To reconstruct the evolutionary history of *Jurinea*, we sampled 187 species representing ca. 77% of the genus diversity covering all distribution areas (see Appendix A for a complete list of species). Plant material was extracted from dried leaves of herbarium collections or field expeditions. Based on previous phylogenetic studies (Susanna et al., 2006; Barres et al., 2013; Herrando-Moraira et al., 2019a), we added 58 outgroup species to estimate the time divergence of *Jurinea* lineages. In total, 245 species were analyzed, from which 131 have been sequenced for the first time in this study and 114 taken from previous ones (Herrando-Moraira et al., 2018, 2019a, 2020; Jones et al., 2019;; Mandel et al., 2014, 2017, 2019).

2.2. Laboratory workflow

We followed the library prep protocol and sequence capture workflow detailed in Herrando-Moraira et al. (2018, 2019a, 2020) based on Compositae COS 1061 loci kit (Mandel et al., 2014) except for the pooling step: here, groups up to eight libraries were arranged (500 ng in total per pool). The final enriched libraries were sequenced using 100 bp paired-end reads in the DNA Sequencing Core CGRC/ICBR of the University of Florida using an Illumina HiSeq 3000 (Illumina, USA) or in Macrogen Co. (Seoul, South Korea) in an Illumina HiSeq 4000 (Illumina, USA). Raw DNA sequence reads were deposited in the NCBI Short Read Archive database (SRA, https://www.ncbi.nlm.nih.gov/sra) under the BioProject accession number PRJNA1013784.

2.3. Target sequence extraction

A first read quality assessment was conducted with FastQC v.0.10.1 (https://www.bioinformatics.babraham.ac.uk/projects/fastqc/). Trimmomatic v.0.36 (Bolger et al., 2014) was used to remove the adapters and clean the reads, and HybPiper v.1.3.1 (Johnson et al., 2016) to extract the target loci. We then removed in downstream analyses all loci flagged as potentially paralogous by HybPiper. Finally, MAFFT v.7.266 (Katoh and Standley, 2013), trimAl v.14 (Capella-Gutiérrez et al., 2009), and FASconCAT-G v.1.02 (Kück and Longo, 2014) were used sequentially to obtain the loci-separated alignments and the concatenated supermatrix. In order to reduce phylogenetic noise, we excluded positions with high substitution rates, following Fragoso-Martínez et al. (2017). However, after removing a total of 6109 positions from the initial supermatrix (159,512 bp), the same unsupported nodes remained (see comparison in Supplementary Fig. 1). Because of that, we used the initial unfiltered dataset in downstream analyses.

2.4. Phylogenetic inference and dating analyses

Phylogenetic inference of *Jurinea* was conducted twice, using concatenation and coalescence methods. For the first method, we performed a maximum likelihood (ML) analysis based on the supermatrix using RAxML-NG (Kozlov et al., 2019) from the CIPRES Science Gateway v.3.1 (Miller et al., 2010). Specifically, we ran a search for the best-scoring ML tree and a slow bootstrap (BS) analysis, with ten randomized and parsimony starting trees and setting each locus as a different partition under the GTR + G nucleotide model. For the BS analysis, we applied the auto-stopping criterion "autoMRE". Branches with BS values >70% were considered as statistically supported (Hillis and Bull, 1993). The resulting tree was visualized with FigTree v.1.4.3 (https://tree.bio.ed.ac.uk/software/figtree/). The coalescence inference was performed with ASTRAL-III v.5.5.3 (Zhang et al., 2018) based on the individual gene trees for each locus previously obtained with a RAxML analysis applying the same settings as for the supermatrix, but with 200 resampling replicates. The local posterior probability (LPP) was used as a branch support metric, considering strongly supported branches with a LPP > 0.95 (Sayyari and Mirarab, 2016).

Due to the large size of the dataset, we used the penalized-likelihood approach implemented in treePL (Smith and O'Meara, 2012) to time-calibrate the best-scoring ML tree obtained with the concatenation approach. We applied the same procedure and calibration points as in Herrando-Moraira et al. (2019a). As a brief description, we obtained the confidence intervals (95% CI) in the estimated node ages running 100 independent treePL analyses with calibration points constrained to a set of random values generated under normal and lognormal distributions, depending on each point (see Herrando-Moraira et al., 2019a). The resultant time-calibrated 100 trees were introduced in TreeAnnotator v.1.7.5 (Drummond et al., 2012) to obtain the maximum clade credibility (MCC) tree chronogram with median node heights and corresponding CIs. This final dated MCC tree is provided in Supplementary Fig. 2.

2.5. Ancestral area reconstructions

To infer the most probable ancestral ranges of *Jurinea* lineages, we performed a biogeographical analysis using the software RASP 4.02 (Yu et al., 2015), which implements the R package *BioGeoBEARS* (Matzke, 2013). As input we used the chronogram tree generated from treePL in which all species other than *Jurinea* were pruned. We defined nine biogeographic areas (see Fig. 1; Supplementary Table 1) according to data on floristic regions (Takhtajan, 1986), biogeographic syntheses of the IT (White and Léonard, 1991; Djamali et al., 2012; Manafzadeh et al., 2017), and global climate delineations (Köppen and Geiger, 1936; Beck et al., 2018). The maximum number of ancestral areas was set to nine.

A first model comparison step was run for the following models: Dispersal–Extinction–Cladogenesis (DEC; Ree et al., 2005), and the likelihood versions of Dispersal–Vicariance (DIVA-like), and BayArea (BAYAREALIKE). The addition of the parameter jump dispersal or founder event speciation "J" (Matzke, 2013) to the models was discarded due to the recently reported possible statistical and conceptual problems derived from its inclusion (Ree and Sanmartín, 2018). The DEC model resulted as the best-fit one according to AIC values (Supplementary Table 2), and thus it was used to compute the final analysis. All models were run under a non-time-stratified analysis and without dispersal multipliers matrix.

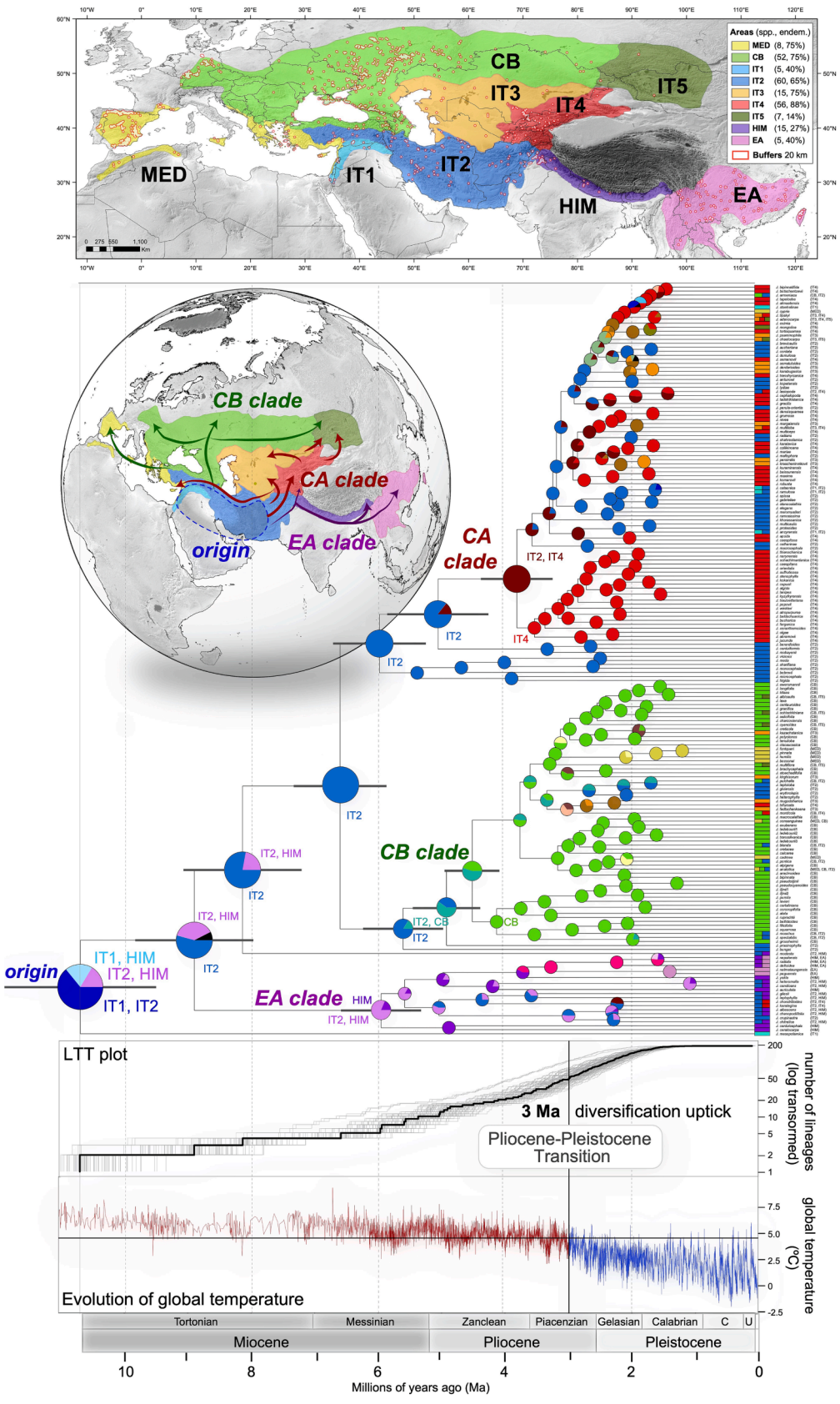

Fig. 1. Distribution of *Jurinea* species diversity (taxa included in the study) across the nine biogeographic areas (justification in supplementary text and descriptions in Supplementary Table S1) and buffer zones, which represent areas around 20 km of each occurrence record (2691 points; Appendix B). Phylogenetic reconstruction of *Jurinea* diversification inferred from the supermatrix of 502 COS loci by maximum likelihood analysis (in RaxML), time-calibrated (in treePL), and reconstructed ancestral biogeographic areas (in RASP, BioGeoBEARS). Colours of tree nodes indicate the most likely estimation of ancestral areas. Tips are also coloured according to the current geographic distribution of each species. Abbreviations of areas for inferred ancestral states are only specified for the main tree backbone nodes, for information about the rest of nodes and all colour correspondence see Supplementary Table S6 and Supplementary Figs. S10 and S11. Gray bars on nodes show the 95% of confidence intervals (CI). The graphs below phylogeny show: the upper one, a lineage-through-time plot (LTT) that indicates the number of lineages emerged (log-transformed) in a temporal line. The black line represents the maximum clade credibility (MCC) tree chronogram and the grey ones correspond to 100 time-calibrated trees. The lower graphic shows the evolution of global mean temperature (°C) since Miocene to present. Abbreviations of areas: MED = Mediterranean; CB = Circumboreal; IT = Irano-Turanian; HIM = Himalayas; EA = Eastern Asia. Abbreviations of time stages: C = Chibanian; U = "Upper".

2.6. Ancestral state reconstruction of growth form

Reconstruction of ancestral growth form was performed on the *Jurinea* chronogram. We classified *Jurinea* species into five growth form categories based on our own observations and descriptions from local floras: (A) annuals with dwarf semiscapose basal rosette; (B) biennials presenting leafy stems with soft and wide leaves; (C) acaulescent perennials; (D) caulescent perennials formed by basal rosettes with leafless flowering stems; and (E) caulescent perennials with leafy flowering stems (see dichotomic diagram in Fig. 2). Inferences about growth form evolution were done using Markov models (Mk) in the R package *diversitree* (FitzJohn, 2012). Four possible discrete Mk models were fitted and compared using AIC values, a null model with different transition rates (ARD) plus three constrained models: a symmetrical model in which transition rate between any two states do not differ (SYM), a symmetrical model with equal rates for the three types of perennial lifeforms (SYM-ERp), and a model with all rates equal (ER).

2.7. Diversification analyses

As a first exploratory analysis, we outlined the accumulation of lineages over time with a lineage-through-time plot (LTT; Nee et al., 1992) with the R package *ape* and function *mltt.plot* (Paradis and Schliep, 2019) setting in log scale axis "y" (number of lineages). As input, we used the maximum clade credibility tree chronogram and the 100 independent dated trees extracted from treePL, which were used to account for the uncertainty of the node age estimations (see details in Herrando-Moraira et al., 2019a).

We investigated diversification dynamics of *Jurinea* following a hypothesis-driven approach to avoid identifiability problems (Louca and Pennell, 2020; Morlon et al. 2022), i.e. we defined a set of diversification models to be fitted and compared in order to test explicit evolutionary hypotheses. Specifically, we tested whether species diversification rates varied (linearly or exponentially) with time, climate, or species-diversity, and included as null models constant-rate ones. Diversity-dependent models include an additional parameter: the clade carrying capacity (K), which corresponds to the number of species that can exist at the same time (Etienne et al., 2012). Concerning diversity-dependent models, we fitted three main types of models: (1) models in which speciation rate was dependent on species-diversity, and a single clade carrying capacity was estimated for the entire study-group; (2) models in which speciation rate also varied with species-diversity, but all estimated parameters were allowed to shift at 3 Ma, with the aim to test for the potential effect of the Pliocene-Pleistocene Transition (PPT) on the net diversification rate and/or the clade carrying capacity; and (3) models in which we allow one of the three main subclades to undergo its own diversification dynamics by enabling a decoupling of diversification rates and clade carrying capacities (Etienne et al., 2012), i.e., the estimated parameters (speciation and extinction rates plus the clade carrying capacity) were separately estimated for the main clade and the decoupled subclade. The latter type of models was fitted to account for the fact that *Jurinea* is composed of three main subclades with different ages and geographical contexts (and thus each subclade may be at a different stage of diversification). We only fitted models allowing variations in speciation rate to avoid potential flaws as indicated by Burin et al. (2019) on models assuming variable extinction rates. To account for incomplete taxon sampling, we applied in each model the analytical correction corresponding to the sampling fraction. The best fitting-model was selected based on AICc. All analyses were run with R packages *RPANDA* (Morlon et al., 2016) and *DDD* (Etienne et al., 2012).

Given that the best-fitting model according to AICc was a diversity-dependent model in which the diversification dynamics of the Eastern-Asian (EA) subclade were decoupled from the main clade, we performed a second round of diversification analyses: we fitted the whole set of models (except those models in which the diversification parameters were decoupled for a particular subclade) to the phylogenetic tree obtained after dropping the EA subclade plus *J. mesopotamica* (hereafter we refer to this subset tree as CB + CA), with the main goal to further investigate the drivers of diversification of the two main subclades that constitute the crown radiation of *Jurinea* (Circumboreal and Central-Asian ones).

2.8. Environmental niche: Data assembly and analyses

To explore the impact of environmental factors in the evolution of main *Jurinea* lineages, we conducted comparative niche analyses. In total, we gathered 2691 records for 158 species, representing 84.5% of our taxon sampling (see Appendix B for the complete list of occurrences and sources). The gathered localities were extracted from several sources: GBIF portal (https://www.gbif.org/), research papers, online floras and atlases, herbarium collections, and virtual herbaria. As environmental predictors, we collected an initial set of 45 variables (at 2.5 arc min or coarser resolutions) related with climate, topography, vegetation, soil properties, habitat heterogeneity, and solar radiation (Supplementary Table 3). We extracted the values of variables for each locality with ArcGIS v.10.2.2 (Esri, Redlands, California, USA 2014). We reduced the initial 45 variables to a set of 21 uncorrelated ones based on the results of a Pearson correlation analysis (Supplementary Fig. 3) and a principal component analysis (PCA) (Supplementary Table 4) to avoid model overfitting. See details of variable selection in Supplementary Information. Two datasets were tested, one with all occurrences and values, and another with the mean values for each species. Given that similar results were obtained (Supplementary Fig. 4C and 4D), we used the mean values as a summary of the species average potential niche.

We identified the variables responsible for niche variation of the main phylogenetic lineages of *Jurinea* through a standard PCA analysis conducted in R v.3.6.3 (R Development Core Team, 2019) using *FactoMineR*, *factoextra* (for PCAs) and *ggplot2*. To test the hypothesis of niche conservatism, expansion, and divergence among lineages, we also conducted the PCA-env analysis designed by Broennimann et al. (2012) with the R script reported in Herrando-Moraira et al. (2019b).

We reconstructed the most probable ancestral niche states with the R function *fastAnc* from *phytools* package (Revell, 2012). As input variables for each species, we used the PC1 and PC2 scores from the standard PCA analysis, and the most variable environmental factors at ancestral nodes or at interspecific level. The changes in environmental values were visualized with the *contMap* function (also from *phytools*).

2.9. Phylogenetic signal in phenotype and environmental variables

We measured the phylogenetic signal of the categorical variable "growth form" with the δ statistic (Borges et al., 2019) computed in R, and of the quantitative variables "altitude" and "environmental niche" (PC1 and PC2 values) with Blomberg's K (Blomberg et al., 2003) computed in RASP. These analyses were performed to discern between non-adaptive radiation (high phylogenetic signal expected, i.e. closely related species present similar phenotype and niche traits), and adaptive radiation (low phylogenetic signal expected, i.e. close relatives exhibit notable differences in trait values).

2.10. Climatic stability inference

We implemented a recently published approach (Herrando-Moraira et al., 2022) to assess the impact of climatic fluctuations on *Jurinea* diversification and to identify stable refugia or unstable climatic areas where the species occur (see schematic overview in Supplementary Fig. 5). In this approach, a Climate Stability Index (CSI) is estimated at a spatial resolution of 2.5 arc min for the period comprised between middle-late Pliocene (3.3 Ma) and the present. To do this, CSI uses the reconstructed paleoclimatic data of the 12 time periods (Supplementary Fig. 5A) included in the PaleoClim database (Brown et al., 2018) representing both warm and cold cycles. The CSI values for each 2.5 arc min

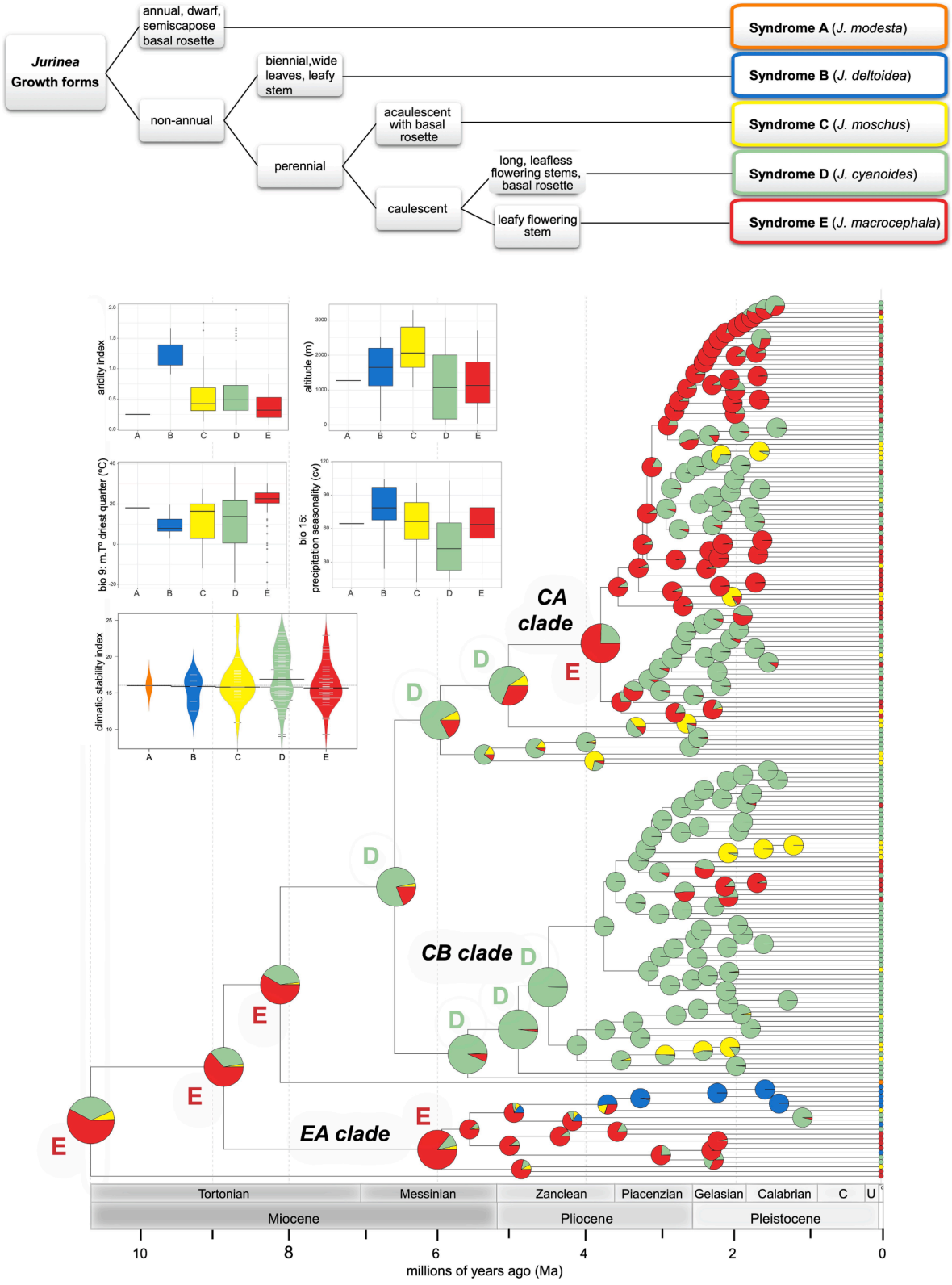

Fig. 2. Results of analyses on growth form evolution. Dichotomic scheme of morphological classification of *Jurinea* according to five main morphological syndromes (coded as A, B, C, D, and E), followed by an example species of each category. For each morphotype, boxplots representing variance of several climate variables based on their current distribution areas (aridity index, bio 9, and bio 15), altitude, and beanplot showing the magnitude of paleoclimatic variation (climatic stability index). Phylogenetic reconstruction of *Jurinea* inferred from the supermatrix of 502 COS loci by maximum likelihood analysis (with RaxML), time-calibrated (with treePL), and reconstructed ancestral morphological syndromes (with *diversitree*). Colours of tree nodes indicate the most likely estimation of ancestral morphologies. Tips are also coloured according to the current morphotype of each species. Abbreviations of growth forms for inferred ancestral states are only specified for the main tree backbone nodes. Abbreviations of time stages: C = Chibanian; U = "Upper".

cell are based on estimating the amount of variation or dispersion along time series by using the standard deviation (Supplementary Figs. 6 and 7; see more details in Herrando-Moraira et al., 2022). The procedure is schematized in Supplementary Fig. 5C. For each species occurrence record, we extracted its corresponding climatic stability index score with the ArcGIS tool "Extract Multi Values to Points". Then, the average was calculated for the species with more than one occurrence to obtain a final dataset with a unique index value per species. Climatic stability data plots were generated with *boxplot* from *graphics* R package and bean plots from portal https://shiny.chemgrid.org/boxplotr/, a web-based R application. The R scripts used for the paleoclimatic analyses are included in Appendix C.

3. Results

3.1. Phylogenetic analyses

From the total 1061 target loci, 502 were finally retained after discarding potential paralogs. The supermatrix resulted in an alignment of 161,485 bp. Phylogenetic reconstruction using concatenation and coalescent-based approaches returned similar topologies at deep tree nodes with strong branch supports (Supplementary Figs. 8–9), except for the position of *J. mesopotamica* Hand.-Mazz. Three main clades were recovered, which mostly corresponded to the three main geographic groups (Fig. 1). Hereafter, we refer to these clades as "Eastern Asia clade" (EA clade), "Circumboreal clade" (CB clade), and "Central Asia clade" (CA clade).

3.2. Divergence times of Jurinea and biogeographic history inference

All numerical results from divergence time and ancestral area estimates are compiled in Supplementary Material: node age values (Supplementary Table 5), corresponding node identifiers (hereafter IDs; Supplementary Fig. 10), probabilities of ancestral areas for each node (Supplementary Table 6; Supplementary Fig. 11) and inferred areas appended to nodes on the phylogenetic tree (Supplementary Fig. 11).

The estimated stem and crown ages for *Jurinea* were 12.8 Ma (11.5–14.5 95% CI) and 10.7 Ma (9.5–12.0), respectively. The most probable ancestral area for the root node of *Jurinea* was IT1–IT2 region (Mesopotamia-Iranian Plateau; Fig. 1). The first main divergence event occurred at 8.9 Ma (7.8–10.0 95% CI) when the EA segregated. In the Messinian period, the EA clade started to diverge at 5.9 Ma (5.2–6.5 95% CI) from an IT2 ancestor, giving rise mainly to Himalayan and East Asian lineages. Subsequent tree backbone nodes showed that the most likely ancestral area was IT2, pointing out that Iranian Plateau was the focal zone of subsequent dispersals to adjacent regions (Fig. 1). In the Miocene-Pliocene transition a second main dispersal occurred to the CB region, which started to diverge around 4.5 Ma (5.1–4.0 95% CI) in a IT2–CB transition, and spread later towards the following regions: IT2, IT3, IT4, IT5, CB, and MED (Fig. 1). Similarly, in the Miocene-Pliocene transition the other main range expansion took place, dated to around 3.8 Ma (3.4–4.6 95% CI) with an ancestral area in IT2–IT4, triggering the origin of the CA clade, which contains lineages that colonized all IT regions, CB, and MED (Fig. 1).

3.3. Growth form evolution

According to AIC values, the best fitting model of growth form evolution was SYM, followed by SYM-Erp ($\Delta AIC = 0.47$; Supplementary Table 7). According to SYM, transitions were most frequent between different types of perennials ($q_{54} = 0.104$, $q_{43} = 0.047$, $q_{53} = 0.037$) than between perennials and biennials/annuals (q values < 0.02). Congruently, according to the second best model, transitions between perennial growth forms were also the most frequent ones ($q_{perennial} = 0.073$). Indeed, most of *Jurinea* species show perennial biotypes. The most heterogeneous group in growth forms was the EA clade, which harboured species with four of the five distinct growth forms (all except annuals) (Fig. 2). Conversely, the CB clade was the most uniform, with type "D" (perennials with leaf rosettes and leafless flowering stems) predominating and with few transitions to types "C" (acaulescent perennials with leaf rosettes) and "E" (subshrubs with leafy flowering stems). The CA clade showed a wide heterogeneity of growth forms (syndromes "C", "D", and "E", being the most abundant the last two), besides exhibiting large disparities among closely related species.

3.4. Diversification analyses

The maximum slope in LTT plot occurred around 3–1.5 Ma (Fig. 1). We compared the fit of 30 models (Supplementary Table 8) and, according to AICc, the best-fitting model was the diversity-dependent one in which the diversification dynamics of the subclade EA was decoupled from those of the main clade. This model indicated that the speciation rate of EA was nearly half of the main clade ($\lambda_{EA} = 0.85$; $\lambda_{main\ clade} = 1.84$) whereas the extinction rate was one order of magnitude higher in EA ($\mu_{EA} = 0.00023$; $\mu_{main\ clade} = 0.00001$). Following this model, EA had reached its clade carrying capacity ($K_{EA} = 25$, which is indeed the estimated current species diversity), whereas the main clade had not yet reached it ($K_{main\ clade} = 342$, while *Jurinea* diversity estimations are of ca. 200 species).

Concerning the diversification models fitted for the CB + CA subset (Supplementary Table 9), the best-fitting model according to AICc was the diversity-dependent model with a major shift of diversification dynamics at the Pliocene-Pleistocene transition (PPT, ca. 3 Ma) and null extinction. This model indicated that the speciation rate nearly doubled after the shift ($\lambda_1 = 0.93$, $\lambda_2 = 1.77$). The estimated values of clade carrying capacity (K) before and after the shift ($K_1 = 6163$ and $K_2 = 331$, respectively) suggested that diversity-dependence developed mainly after PPT. The ΔAIC between the best and second-best model was above the threshold of 2, which is typically chosen to discern models with confidence for both datasets (all *Jurinea* and CB + CA subset).

3.5. Phylogenetic patterns in environmental variables

Environmental variables that mainly contributed to the separation of the phylogenetic clades were aridity (12.8% of contribution to PC1 axis of standard PCA) and altitude (19.2% in PC2 axis; Fig. 3A–3B; Supplementary Table 10). In the present study case, altitude was highly correlated (Pearson's $r > 0.4$) with soil quality and other topographic variables (Supplementary Fig. 2). Standard PCA (Fig. 3B) and PCA-env (Supplementary Fig. 3B) analyses revealed that species environmental niches of the three main clades (EA, CB, and CA) overlap considerably (D = ca. 30%; Supplementary Table 11). The clade EA showed the highest niche breadth and turned out to be equivalent to niches found in CB and CA (p-value < 0.05; Supplementary Table 11). Comparing the three main clades, the CB showed high niche expansion values with respect to the other two clades (33% with respect to EA and 41% with respect to CA; Supplementary Table 11).

Ancestral reconstruction of the first two PC axes (Fig. 3C) showed that CB clade was the one including species with most diverging niches. Our results indicated that the majority of *Jurinea* species are present in territories with an aridity index < 0.5, which corresponds to drylands according to the criterion of Middleton & Thomas (1997); the species found in humid zones (aridity index > 0.65) were mostly clustered in the CB and EA clades (Fig. 4). All the species from Caucasus (which constitute a single subclade of 14 species within the CB clade) were found in humid or sub-humid areas (aridity index ≥ 0.5; Fig. 4). Regarding altitude, the majority of species (57%) of the CB clade are found at low elevation (<1000 m). In contrast, EA and CA clades present a much lower proportion of low altitude species (14 and 33%, respectively).

Statistically significant levels of phylogenetic signal (Blomberg's $K > 1$; p-value = 0.001) were recovered only in CB clade for environmental

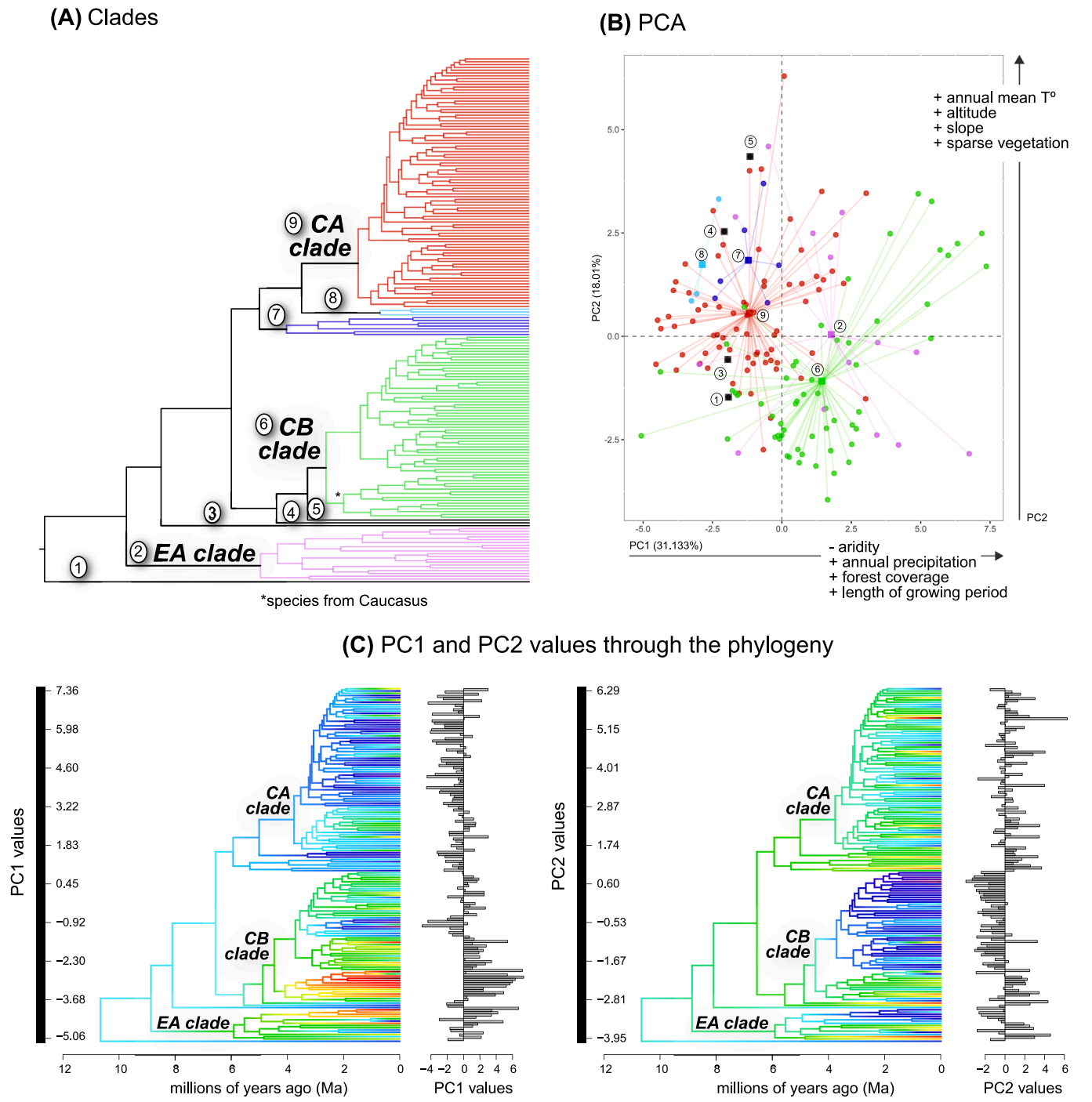

Fig. 3. (A) Classification of clades (see Fig. 1). (B) Graphical output of Principal Component Analysis (PCA) analysis of the values of 21 climatic variables for each species, representing the global environmental space and the distribution of each phylogenetic group. (C) Ancestral state reconstructions (obtained with the *fasAnc* function of R package *phytools*) of PC1 and PC2 scores for each species, representing the ecological niche evolution along the phylogenetic history of *Jurinea*. Loading values for each species of both PCs are represented in vertical barplots besides the time-calibrated phylogeny.

niche and altitude. The δ-value related to growth form conservatism was also three-fold higher in CB than for the other clades (Table 1).

3.6. Paleoclimatic oscillations and long-term stable regions

Paleoclimatic data analyses identified both climatic stable refugia and highly variable regions along IT and surrounding territories (Figs. 5–6). We detected local stable climatic conditions since middle-late Pliocene to present in the Mediterranean region, Anatolia, Mesopotamia, Iranian Plateau, central-eastern Himalayas, and south-eastern Asia. As a general pattern, climatic fluctuations affected the northernmost areas (especially for temperature oscillations) and East Asia (especially for precipitation; Fig. 6). Accordingly, the CB clade, which has more northerly distributed species, showed higher median and range values (Q1–Q3) of climatic stability index (Fig. 7A; Table 1), i.e. species occur in regions that had more unstable climate. The top species rich-areas (IT2, IT4, CB) showed medium–high values of climatic oscillations (Fig. 7B).

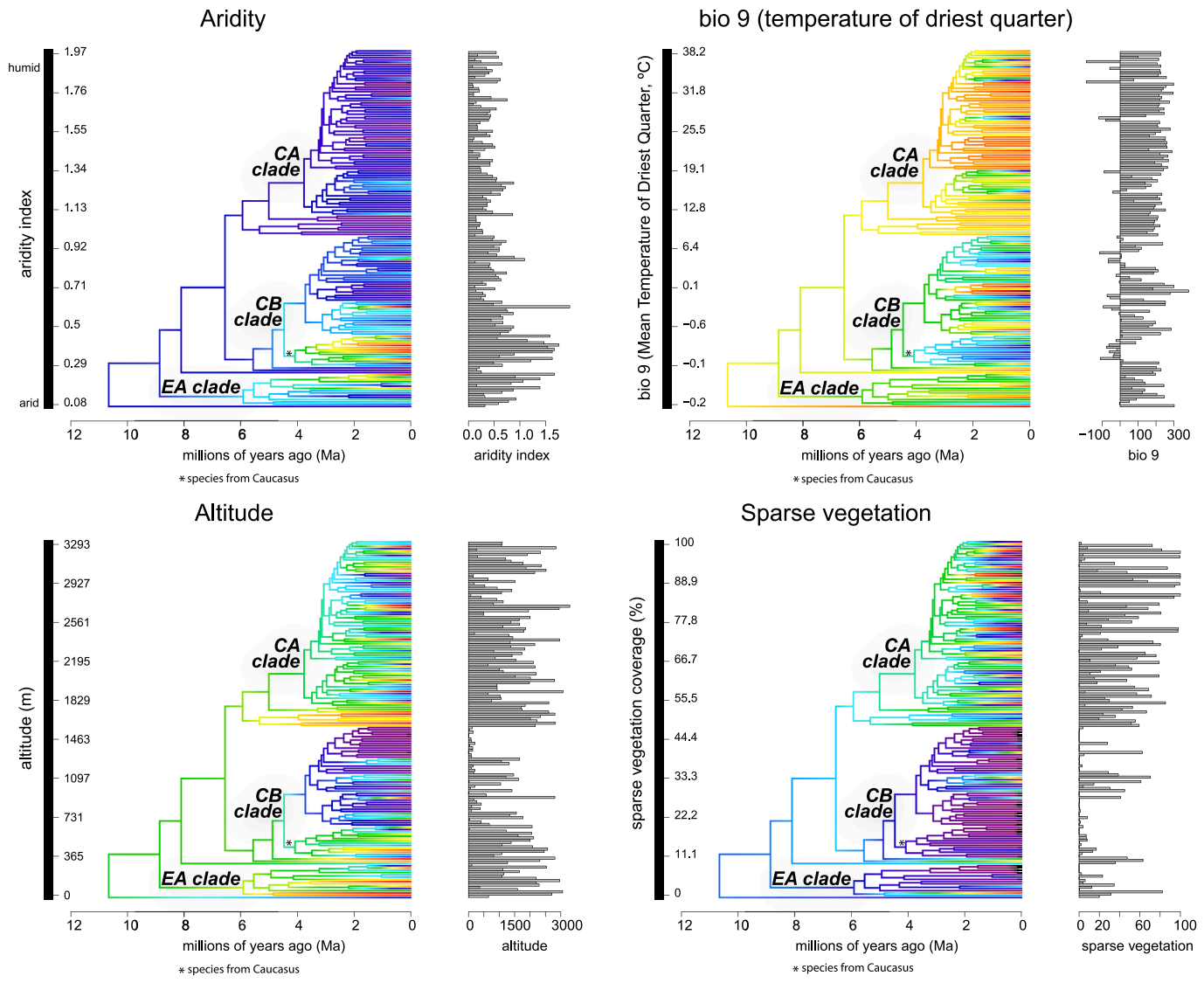

Fig. 4. Estimation of ancestral states reconstructed with the *fasAnc* function of R package *phytools* for the most variable environmental traits across the *Jurinea* phylogeny. Loading values for each species are represented in vertical barplots besides the time-calibrated phylogeny. The asterisk indicates the clade containing species exclusively found in the Caucasus.

4. Discussion

The present study offers new evidence on the tempo, mode, and drivers of evolution of the IT flora, which is one of the least studied Eurasian floras despite its high diversity and rate of endemism. The integrative approach applied here, combining data from multiple sources (phylogeny, biogeography, geology, ecology, morphology, and paleoclimate), revealed the importance of climate shifts and topographic heterogeneity as triggers or modulators of species radiations. Importantly, the paleoclimatic analyses highlighted that either long-term climatic stability or moderate climate oscillations could explain high species richness in two biogeographic regions depending on their general topography. In the Iranian Plateau, the high climatic stability detected would explain its high richness of xerophytic elements and its role as a museum and a cradle for the IT flora. Contrarily, regional climatic fluctuations in the Circumboreal region and mountains of Central Asia fostered allopatric diversification, especially in lineages adapted to semi-arid and cold areas.

4.1. Cold-arid climatic conditions as triggers of Jurinea radiation

The main evolutionary events of *Jurinea* were probably substantially influenced by climate-related turnovers, especially those that led to colder and drier conditions: (1) the origin of the genus (10.7 Ma; Fig. 1) occurred during a major global climate change, turning from warm-tropical and subtropical to cool-temperate conditions at the onset of global cooling and marked seasonality during mid-late Miocene (Potter and Szatmari, 2009; Pound et al., 2012; Herbert et al., 2016); (2) long-distance dispersals from IT to other floristic regions (~7–4 Ma; Fig. 1) occurred around the Miocene-Pliocene boundary, a period characterized by global biotic turnovers (LaJeunesse, 2005), such as the expansion of C4 grasslands (Shen et al., 2018) in response to a major cooling trend between 7.0 and 5.5 Ma (Holbourn et al., 2018) and the aridification of Central Asia (Miao et al., 2012); and (3) diversification dynamics of the main lineages of *Jurinea* (i.e., the CB and CA clades) suffered a significant diversification shift during the Pliocene-Pleistocene Transition (ca. 3 Ma; Fig. 1), in which the net diversification rate almost doubled, from $\lambda = 0.93$ to $\lambda = 1.77$. During this later period, climate turned colder and drier at the onset of the Northern Hemisphere glaciations when large continental ice sheets appeared, resulting in important environmental

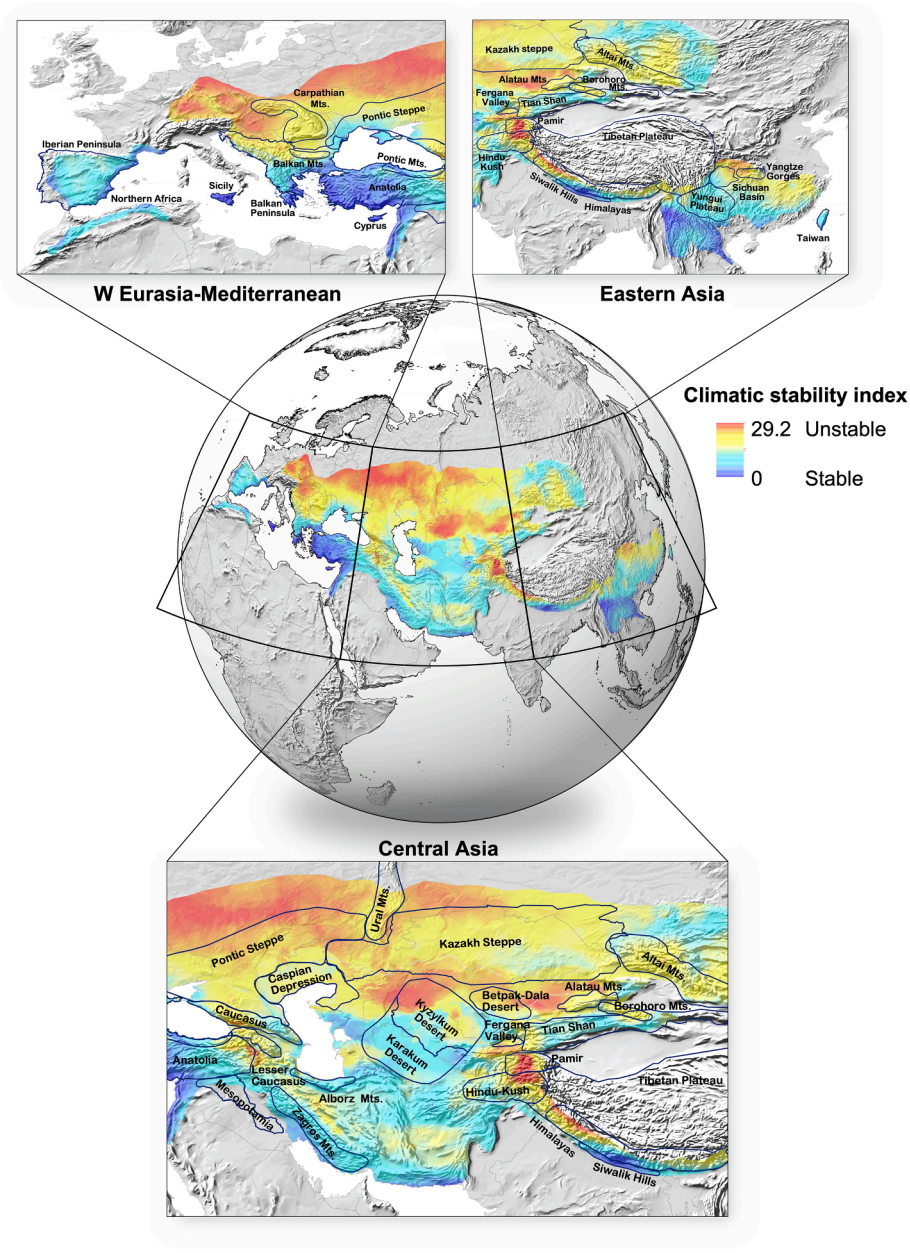

Fig. 5. Mapped values of climatic stability index (CSI) for the study area from Pliocene (3.3 Ma) to present, at a resolution of 5 × 5 km. Colours range from blue for low standard deviation (SD) values, which represent areas with low climatic fluctuations from Pliocene to present, to red for high SD values, which show areas where high climatic fluctuations probably took place. Main geographic locations (e.g. mountains, deserts) are indicated in the zoomed maps. This index is based on data from six variables (bio1 = annual mean temperature; bio4 = temperature seasonality; bio9 = mean temperature of driest quarter; bio12 = annual precipitation; bio15 = precipitation seasonality; and bio17 = precipitation of driest quarter). (For interpretation of the references to colour in this figure legend, the reader is referred to the web version of this article.)

changes (Willeit et al., 2015). Lineages that could not adapt to novel environments either dispersed to suitable habitats or faced extinction. *Jurinea* seems to have taken evolutionary advantage of these climate shifts towards dry-cold regimes. The diversification increase detected for the last 3 million years could be related to geographic range modifications or to adaptation to these new ecological opportunities and niches deserted by other plant groups unable to adapt to plummeting temperature and precipitation. Indeed, during this period *Jurinea* lineages also showed an increasing trend of form lability (Fig. 2) and ecological niche shifts (Figs. 3–4), probably as an adaptation to novel habitats and new geographic areas. Overall, *Jurinea* is an excellent example of the extensive impact of gradual global cooling trend over the past 15 Ma on diversification history and expansion of the temperate biota of the Northern Hemisphere (Folk et al. 2019, 2020 and references therein).

4.2. *Insights into evolutionary and biogeographic hypotheses on the Irano-Turanian flora*

In relation to the temporal origin of typical xerophytic species within the IT, we found that *Jurinea* originated in the middle-late Miocene, ca. 10.7 Ma (9.5–12.0; Fig. 1), a more recent origin than that suggested for the IT elements (Manafzadeh et al., 2017). Spatially, *Jurinea* started to diverge in Western Asia around Mesopotamia and the Iranian Plateau (region IT1–IT2 here; Fig. 1). Within IT, Western Asia is a centre of origin for numerous plant radiations that also occurred during middle-late Miocene (Barres et al., 2013; Karl and Koch, 2013; Lauterbach et al., 2019; Peterson et al., 2019). The definitive closure of the Mesopotamian Seaway in the middle Miocene at 13.8 Ma (Bialik et al., 2019) could have promoted this deep-lineage divergence, as new lands to be colonized were available (Potter and Szatmari, 2009; Herbert et al., 2016).

The colonization of adjacent regions by IT elements could be the result of independent dispersion waves. In *Jurinea*, the first colonized

Table 1
Summary of main results of five key questions in *Jurinea* radiation. Species formation and growth form transition processes were calculated according to retention (same inferred area or habit) or shift in internal nodes and tips respect their respective MRCA node. Abbreviations: BS = bootstrap; E-C = expansion–contraction model; IT = Irano-Turanian; LPP = local posterior probability; MRCA = most recent common ancestor; p% = probability in percentage; Phy-signal = phylogenetic signal; spp = species; SS = strong significant phylogenetic signal.

Specific attributes or measurable traits	*Jurinea* (whole tree)	Eastern Asia (EA clade)	Circumboreal (CB clade)	Central Asia (CA clade)
Number of species	187	19	65	89
Estimated sampling fraction	77%	68%	74%	67%
Clade support (BS/LPP)	100/1	100/1	100/1	100/1
Divergence time (crown age)	Late Miocene (10.7 Ma)	Late Miocene (5.9 Ma)	Pliocene (4.5 Ma)	Pliocene (3.8 Ma)
Ancestral areas (p%)	IT1–IT2 (64%)	IT2–HIM (81%)	IT2–CB (55%)	IT2–IT2 (100%)
Species formation process	*in situ* (60%)	colonization (76%)	*in situ* (70%)	*in situ* (57%)
Geographic scale (spp/km^2)	5.9×10^{-6}	1.9×10^{-6}	3.3×10^{-6}	11.1×10^{-6}
Growth form conservation or transition	conservation (81%)	conservation (64%)	conservation (90%)	conservation (78%)
Phy-signal growth form: δ	6.21	1.33	18.89 SS	4.15
Phy-signal niche PC1: K	0.58	0.78	1.29 SS	0.80
Phy-signal niche PC2: K	0.52	0.96	1.19 SS	0.74
Phy-signal altitude: K	0.53	0.62	1.22 SS	0.75
Climatic stability index:median (Q1-Q3)	16.05(14.70–18.68)	16.20(15.60–17.35)	17.8(14.63–20.70)	15.9(14.8–18.0)
Radiation type proposed	Mixed model	Adaptive	Non-adaptive	Adaptive
Diversification drivers and history	- Climate changes - Pre-adaptation to aridity- Geographic speciation (longitudinal, latitudinal, altitudinal)	- Niche partitioning on ecologically constrained adaptive landscapes- Low evolutionary potential in mesic habitats	- Range and niche shift towards humid conditions - Niche conservatism- Climatic oscillations stimulated allopatric speciation	- Climate fluctuations and orogeny in Pamir-Tian Shan mountains- Growth form and niche lability fostered local adaptation

region out of IT was East Asia (late Miocene), the second the Circumboreal region (Pliocene), and the last one the Mediterranean region (Pleistocene), which was colonized repeatedly by different clades (Fig. 1). Among these regions, the genus notably diversified only in the Circumboreal region, whereas in Eastern Asia the net diversification rate was significantly lower than in other regions. Internal movements and range expansions between IT areas (IT1-IT5) occurred during the Pliocene-Pleistocene boundary.

4.2.1. *The Iranian Plateau as both a museum and a cradle for plant diversity*

Our results suggest a double role of the Iranian Plateau as a "museum" (old-lineage persistence) and a "cradle" centre (*in situ* speciation; cf. Moreau and Bell, 2013) for *Jurinea*, which has also been documented for other IT radiations such as *Acantholimon* (Moharrek et al., 2019). For instance, most of the deepest nodes of *Jurinea* were distributed in this area, according to our biogeographic estimations; in contrast, some recent nodes gave rise to several endemics (Fig. 1). The dual role of this region as a museum and a cradle is likely linked to one of our main findings: here we demonstrated for the first time that the Iranian Plateau is a region characterized by long-term high climatic stability (Figs. 5 and 7B), one of the main causes determining high species richness and endemism of world's biodiversity hotspots (Harrison and Noss, 2017). Specifically, our analysis of paleoclimatic data revealed a low temporal variation in IT2 for annual precipitation and, particularly, precipitation of driest quarter (bio 12 and bio17, respectively; Fig. 6; Supplementary Fig. 6); thus, the precipitation regime remained rather constant since the Pliocene, without abrupt regional changes even during the periods of strongest climatic changes such as the LGM (time "5" in Fig. 6; Supplementary Fig. 5). This factor probably favoured the persistence of *Jurinea* species as well as other xerophytic IT elements.

Takhtajan's (1986) old hypothesis is once again verified here: the IT flora originated along the Iranian Plateau and served as biodiversity source for the adjacent regions. For some millions of years during late Miocene (ca. 10.7–6 Ma) *Jurinea* probably remained within the Iranian Plateau (Fig. 1). Its diversification was constant during the so-called period of the "Pikermian chronobiome", when arid-seasonal climates and open environments dominated in Eurasia (Hurka et al., 2019). The main transregional dispersal events took place around 6–4 Ma during the Miocene-Pliocene transition, when the genus successfully colonized three geographic areas: East Asia, the Circumboreal region, and Central Asia. This period is coincident with an intense phase of uplift and deformation along the Iranian mountain ranges: Zagros, Alborz, and Kopeh Dagh (Mouthereau, 2011), which provided isolated geographic areas that promoted allopatric speciation, as well as new habitats that created opportunities for ecological speciation. It is also coincident with the onset of the Central Asia aridification (7–5.3 Ma; Sun et al., 2015) and a phase of intense cooling in Northern Hemisphere (the "Late Miocene Cooling"; 7–5.4 Ma; Zachos et al., 2001; Herbert et al., 2016). These climatic changes likely led to a decrease in native competitors and herbivores as shown by the regional extinction events of mammalian biochronological indicators (Casanovas-Vilar et al., 2010, 2011; Ge et al., 2012). Consequently, new lineages as *Jurinea*, other xerophytic plants and C4 grasses (Huang et al., 2007; Arakaki et al., 2011) could have spread as a result of antagonists decrease (Yoder et al., 2010) and their pre-adapted niches to arid habitats. Here, we confirmed the pre-adaptation hypothesis based on the phylogenetically conserved values obtained for aridity (Fig. 4), which may have resulted in higher rates of successful establishment in new available areas by *Jurinea* lineages

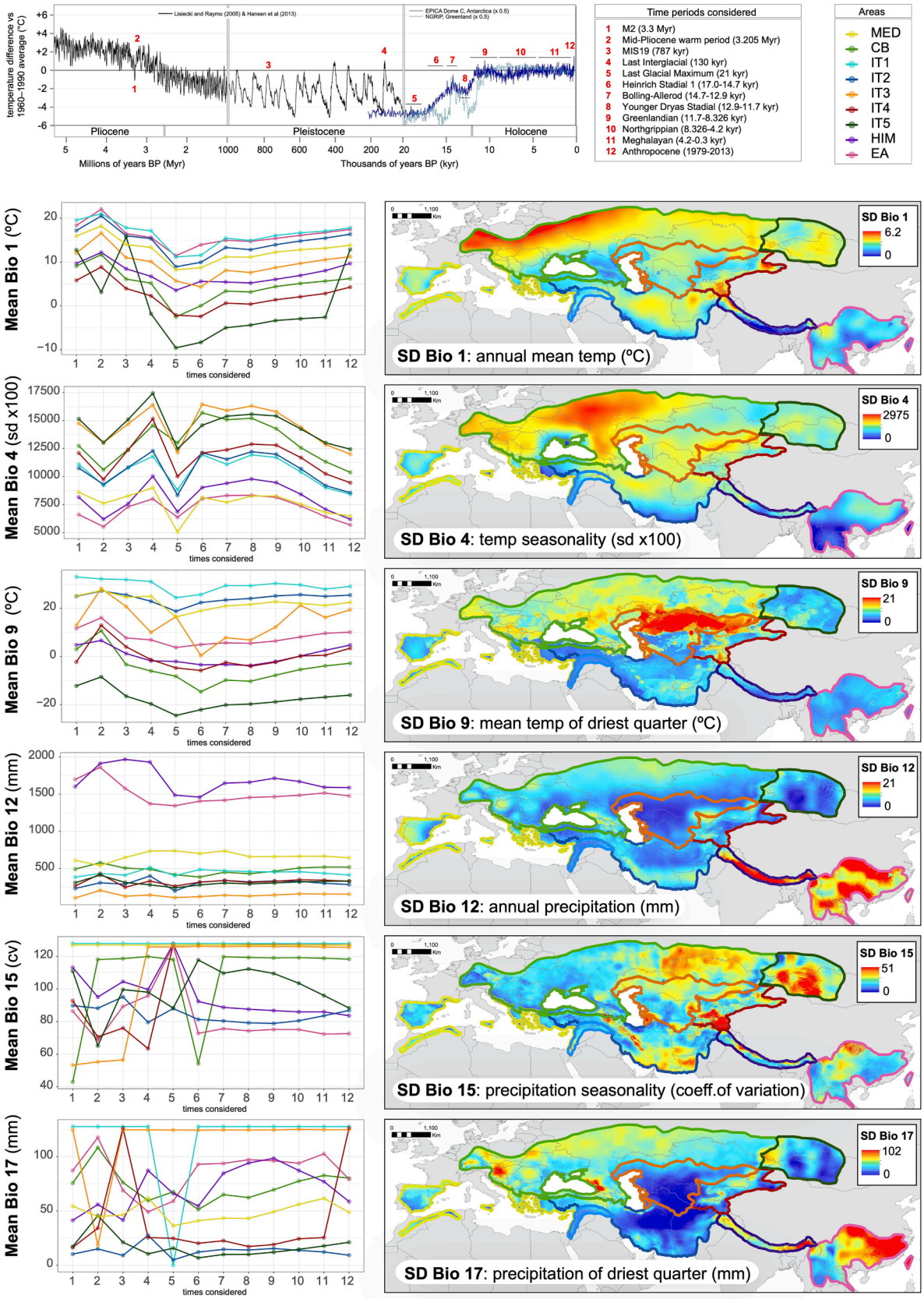

Fig. 6. Representation of climatic variable oscillations through the 12 time intervals (see Supplementary Fig. S5) of PaleoClim dataset (Brown et al. 2018), as implemented in Herrando-Moraira et al. (2022). On the left, we show values for temperature variables (bio1, bio4, bio9) and precipitation variables (bio12, bio15, bio17) for each of the nine biogeographic areas defined. On the right, for each variable and biogeographic area, the standard deviation (SD) along the 12 time periods considered is mapped. The upper panel shows the evolution of global temperature since the Pliocene compared to the average temperature during the period 1960–1990.

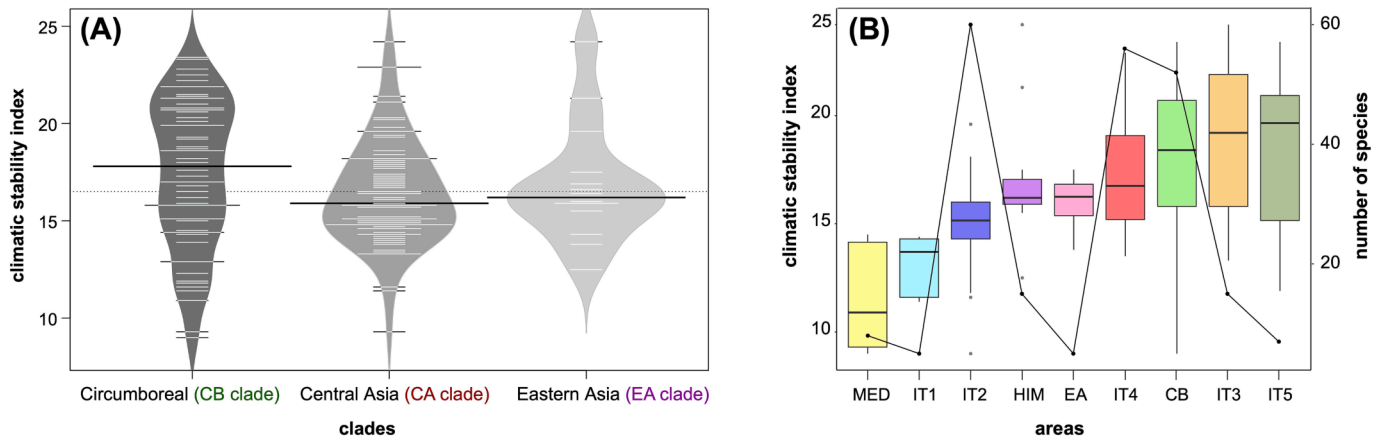

Fig. 7. Plots showing range of climatic stability index values for (A) the three main clades and (B) the nine biogeographic areas (see Fig. 1) based on mean index values for each species. The graphical representation type is a beanplot in (A), in which white lines represent species values, and a boxplot in (B) with a superposed line showing the species richness for each region.

(Peterson, 2003), as documented in alpine radiations by cold-adapted lowland clades (Uribe-Convers and Tank, 2015; Ye et al., 2019).

4.2.2. *Successful dispersal pathways and geographic dead ends*

The first dispersal of *Jurinea* out of IT occurred at 5.9 Ma and led to the emergence of EA clade, extending the genus from the Iranian Plateau towards the Himalayas (probably across the mountain ranges connecting IT2 and HIM), Central Asia Mountains (IT4), and East Asia (subtropical China, Myanmar, Vietnam, and Taiwan). A similar dispersal corridor has been postulated for other IT elements (e.g. *Gagea* Salisb. [Liliaceae], Peterson et al., 2019) but, as in *Jurinea*, this dispersal event originated a species-poor clade. Later, we discuss hypotheses that could explain why some IT elements found a dead end along this East Asia corridor.

During the Miocene-Pliocene transition, early diverging clades that coexisted in the Iranian Plateau gave rise to CB (at 4.9 Ma) and CA clades (at 3.8 Ma), both of which colonized large parts of Eurasia (Fig. 1). The CB clade is comprised of two main subclades that are highly differentiated in terms of geographical expansion. One subclade contains species exclusively found along the Caucasus mountains, which corresponds to a known radiation of ca. 20 endemic species (Szukala et al., 2019). The other one is much more widespread geographically, as it includes species distributed through vast CB territories (i.e. N Anatolia, Balkan Peninsula, the river basins of Dnieper, Don, and Volga rivers, the Caspian Depression, and South-Central Russian uplands). Moreover, back-colonizations to IT2 and dispersal towards other IT regions (IT3, IT4 and IT5) also occurred within this subclade. Two main causes may account for the poor diversity of these IT lineages: (1) founder effects associated with long distance dispersal, which implies low potential genetic plasticity to adapt to a new environmental space; or (2) high climatic instability of most of the newly colonized areas (especially in IT3 and IT5 regions; Figs. 5–6) that would have increased local extinction rates. These areas were later recolonized by recently-diverged *Jurinea* lineages, whose recent origin could explain the absence of large *in situ* radiations.

Jurinea also colonized the Mediterranean Basin several times during the Pleistocene, coincident with the oldest xeric period of the region and the emergence of Mediterranean-type vegetation (ca. 2.3 Ma, Suc, 1984). Such transregional dispersal is responsible for the so-called "Kiermack disjunctions" between western Mediterranean and Central Asia (Ribera and Blasco-Zumeta, 1998). Contrary to other IT elements that actively diversified in the Mediterranean (Banasiak et al., 2013; Manafzadeh et al., 2014; Peterson et al., 2019), this region did not become a secondary speciation centre for *Jurinea* (only ca. 6 endemic species are known), as it would be expected for a long-term climatically stable area (Harrison and Noss, 2017). Reasons are probably two-fold: on the one hand, species of *Jurinea* reached the Mediterranean only in the Pleistocene, a too short time for a radiation to occur. On the other hand, Mediterranean vegetation would have been well-established at the arrival of the *Jurinea* ancestral taxa and, thus, with a low availability of empty niches.

The route towards Central Asia (CA clade) was established during the Pliocene (at ca. 3.8 Ma). Members of this clade reached all IT regions, and even the Mediterranean region at least once (*J. cypria* Boiss., a near-endemism of Cyprus, belongs to the CA clade). More than half of *Jurinea* sampled species originated within this successful lineage. Unfortunately, a fine-scale discussion about the biogeographic history of this lineage is hindered by low support values recovered within CA clade (Supplementary Fig. 7–8). Further exploration of another type of high-throughput molecular markers may be necessary to unravel the CA radiation. COS target loci, which are conserved orthology loci identified from expressed sequence tags (Mandel et al., 2014), do not seem the most adequate markers for disentangling rapid species radiations when incomplete lineage sorting and contradictory signals among coding sequences occur, as is probably the case for the CA clade. Such pattern of conflicting gene information has also been suggested for the radiation of Andean *Lupinus* L. by Nevado et al. (2016), who found that over 40% of genes had undergone adaptive evolution of coding sequences.

4.3. *Parallel and independent diversification scenarios of three Jurinea lineages*

Given that the three main clades (EA, CB, and CA) followed independent evolutionary histories and were probably driven by distinct extrinsic forces, we separately discuss their diversification dynamics below.

The CB clade, dominated by circumboreal taxa, contains 65 species, representing 35% of the total explored richness. It originated with the expansion of *Jurinea* from IT2 to CB region ca. 4.5 Ma, coinciding with a climate reversal from cool to warm-humid conditions known as the "Pliocene climatic optimum" (Sniderman et al., 2016; Jiménez-Moreno et al., 2019) that probably facilitated northward expansions. In the first stages of diversification of the CB clade, ecological speciation may have prevailed, given the wide range of ecological niche diversity detected at the tree backbone in the CB clade (Figs. 3–4). Later, such ecologically divergent lineages further diversified, probably through allopatric speciation given the high phylogenetic signal recovered for niche, growth form, and altitude of CB clade (Table 1; Fig. 4). Indeed, the CB clade harbours a high number of species growing in regions that have been climatically unstable from the Pliocene to present (Figs. 5 and 7A).

Drastic climatic oscillations in the circumboreal region during the Pleistocene probably lead to repeated cycles of range expansion and contraction that fostered further diversification, as shown for other floras (e.g. Winkworth et al., 2005).

The diversification of the Central Asian clade, the most species-rich lineage of *Jurinea* (89 species, ca. 50% of total richness), was probably triggered by a combination of climatic and orogenic factors. During the cold-arid period in the Asian interior dated to 3.6 Ma (Rea et al., 1998; An et al., 2001; Zheng et al., 2004), plant communities experienced marked turnovers to drought tolerant taxa (An et al., 2005; Koutsodendris et al., 2019). Congruently, we observed niche changes towards adaptation to higher aridity and open habitats in the origin of CA clade (Fig. 4), and a growth form reversion to the most ancestral habit (syndrome "E", foliose subshrubs; Fig. 2), likely as an adaptation to arid climates in the Mesopotamian-Iranian region (IT1–IT2; Fig. 1). Therefore, aridity could have acted as a speciation stimulus to CA radiation (Stebbins, 1952). Speciation was also probably fostered by orogenic processes in Central Asia resulting in new habitats. The Pamir-Tian Shan convergence began at ca. 3–5 Ma (Fu et al. 2010; Thompson et al. 2015) when Pamir advanced about 300 km northwards (Burtman and Molnar, 1993; Burtman, 2000), and parallel and subsequent pulses of deformation and rapid uplifts of Pamir-Tian Shan mountain belts occurred (Zhang et al., 2013). We hypothesize that CA ancestors diverged ecologically and occupied multiple habitats provided by mountain ranges, partitioning their niche along altitudinal gradients differentiated by topography, microclimate, predator pressure, pollinators, soils, or vegetation structure (Karl and Koch, 2013; Seehausen, 2015; Sundue et al., 2015). This is supported by (1) the lack of phylogenetic signal detected for the global niche and the altitude variable, indicating niche divergence between sister species (Figs. 3 and 4, Table 1), and (2) growth form lability (Fig. 2; Table 1), which likely enabled rapid adaptation to new environments. Overall, the diversification of CA shows signs of adaptive radiation such as high morphological disparity and weak niche conservatism (Stroud and Losos, 2016). However, we suggest that diversification was also fostered by geographical isolation processes given the high climatic oscillations detected in Pamir/S Tian Shan area (Figs. 5 and 6), which probably induced altitudinal and/or latitudinal migrations.

The EA clade is the oldest and most species-poor one. In the biogeographic history of *Jurinea*, the Himalayas acted as a bridge between two climatic and floristic regions: the continental, summer-dry Irano-Turanian and the summer-monsoon East Asian regimes (Takhtajan, 1986; Djamali et al., 2012). However, *Jurinea* did not explosively radiate in either the Himalayan corridor or in East Asia (Fig. 1; Table 1), remaining there as a relatively depauperate lineage despite showing wide ecological niche breadth (Figs. 3 and 4) and high morphological disparity (Fig. 2; Table 1). The low speciation rate detected (half of CB and CA clades) could be the result of the fact that the suitable adaptive landscape space was already almost filled when *Jurinea* arrived. Examples of successful "native" competitors would be the closely-related, species-rich genus *Saussurea* DC., and other evolutionary successful groups such as *Delphinium* L. and *Pedicularis* L. (Wen et al., 2014). Given its xerophytic ancestral background, *Jurinea* might not present enough evolutionary potential to successfully diversify in humid environments. Analogous cases exist in two sister subtribes of Cardueae, Arctiinae and Onopordinae (Herrando-Moraira et al., 2019a). In Arctiinae, the explosive radiation of the mostly xerophytic *Cousinia* Cass. (ca. 600 spp.) in the IT region contrasts with the depauperate genus *Arctium* L. (27 spp.), which is mainly adapted to mesophilous habitats (López-Vinyallonga et al., 2009; Susanna and Garcia-Jacas, 2009). The subtribe Onopordinae shows a lineage with greater success in xeric habitats (*Onopordum* L., 60 spp.), in contrast to seven small genera in the mesic habitats of CA (*Alfredia* Cass., *Ancathia* DC., *Lamyropappus* Knorring & Tamamsch., *Olgaea* Iljin, *Syreitschikovia* Pavlov, *Synurus* Iljin, and *Xanthopappus* C.Winkl.).

5. Conclusions

We focused on the radiation of *Jurinea* as a proxy to understand the evolutionary assembly of the Irano-Turanian flora. Our results depict a dual role of the Iranian Plateau for plant diversity both as a museum and cradle region, in which long-term climatic stability favoured old-lineage persistence. This region has constituted an important source of xerophytic lineages for other Eurasian hotspots such as the Mountains of Central Asia, where *Jurinea* highly diversified. *Jurinea* illustrates that large plant radiations can be the result of both adaptive and non-adaptive processes (Donoghue and Sanderson, 2015). Indeed, *Jurinea* is constituted by three main clades whose diversity results from different macroevolutionary scenarios. The Circumboreal lineage is probably the result of a non-adaptive radiation, in which allopatric processes predominated as a result of high climatic instability of the region during the Pleistocene. In contrast, the Central Asian and the East Asian clades often show divergent ecological niches and high growth form disparity among closely related species. The evolutionary success of the Central Asian clade (the most diverse one) is probably both due to geographical isolation as well as new ecological opportunities provided by orogenic processes in the Pamir-Tian Shan mountains occurred since the Pliocene. Moreover, in this region, predominating cold and arid conditions during the Pleistocene likely favoured preadapted taxa as is the case of *Jurinea*. Contrarily, the East Asian clade is the most species-poor one, probably as a result of the low evolutionary potential of *Jurinea* in mesic habitats. In sum, the radiation of *Jurinea* resulted from the combined action of climatic, orogenic and ecological factors occurring at different temporal scales, showing that large radiations are not the result of a single factor.

CRediT authorship contribution statement

Sonia Herrando-Moraira: Investigation, Data Curation, Formal analysis, Visualization, Writing – original draft. **Cristina Roquet:** Formal analysis, Writing – original draft, Writing – review & editing. **Juan-Antonio Calleja:** Resources, Writing – review & editing. **You-Sheng Chen:**Resources. **Kazumi Fujikawa:** Resources. **Mercè Galbany-Casals:** Conceptualization, Investigation, Supervision, Writing – review & editing. **Núria Garcia-Jacas:** Conceptualization, Supervision, Writing – review & editing. **Jian-Quan Liu:** Resources, Investigation. **Javier López-Alvarado:** Resources. **Jordi López-Pujol:** Formal analysis, Funding acquisition, Writing – review & editing. **Jennifer R Mandel:** Formal analysis, Writing – review & editing. **Iraj Mehregan:** Resources. **Llorenç Sáez:** Writing – review & editing. **Alexander N Sennikov:** Resources, Investigation. **Alfonso Susanna:** Conceptualization, Supervision, Funding acquisition, Writing – review & editing. **Roser Vilatersana:** Resources. **Lian-Sheng Xu:** Resources, Investigation

Declaration of Competing Interest

The authors declare that they have no known competing financial interests or personal relationships that could have appeared to influence the work reported in this paper.

Data availability

Data will be made available on request.

Acknowledgements

Authors thank Maria Luisa Gutiérrez, Fernando Castro, and Laia Barres for providing technical support during the laboratory process. We also thank the herbaria that provided material for the study: BC, DUSH, E, FRU, GDA, H, LE, MBK, MEM, MHA, MO, MU, OS, SANT, TAD, TARI, TI, TK, US, W, and WU. We gratefully acknowledge the University of Memphis computing facilities to allow us the utilization of its high-

performance cluster (HPC). We also acknowledge funding support from the Ministerio de Ciencia e Innovación (Project CGL2015-66703-P MINECO and Ph.D. grant to Sonia Herrando-Moraira) and the Catalan government ("Ajuts a grups consolidats" 2017-SGR1116 and 2021SGR00315).

Appendix A. Supplementary data

Supplementary data to this article can be found online at https://doi.org/10.1016/j.ympev.2023.107928.

References

An, Z., Kutzbach, J.E., Prell, W.L., Porter, S.C., 2001. Evolution of Asian monsoons and phased uplift of the Himalaya-Tibetan plateau since Late Miocene times. Nature 411, 62–66.

An, Z., Huang, Y., Liu, W., Guo, Z., Clemens, S., Li, L., Prell, W., Ning, Y., Cai, Y., Zhou, W., Lin, B., Zhang, Q., Cao, Y., Qiang, X., Chang, H., Wu, Z., 2005. Multiple expansions of C4 plant biomass in East Asia since 7 Ma coupled with strengthened monsoon circulation. Geology 33, 705.

Arakaki, M., Christin, P.A., Nyffeler, R., Lendel, A., Eggli, U., Ogburn, R.M., Spriggs, E., Moore, M.J., Edwards, E.J., 2011. Contemporaneous and recent radiations of the world's major succulent plant lineages. Proc. Natl. Acad. Sci. USA 108, 8379–8384.

Banasiak, Ł., Piwczyński, M., Uliński, T., Downie, S.R., Watson, M.F., Shakya, B., Spalik, K., 2013. Dispersal patterns in space and time: a case study of Apiaceae subfamily Apioideae. J. Biogeogr. 40, 1324–1335.

Barres, L., Sanmartín, I., Anderson, C.L., Susanna, A., Buerki, S., Galbany-Casals, M., Vilatersana, R., 2013. Reconstructing the evolution and biogeographic history of tribe Cardueae (Compositae). Am. J. Bot. 100, 867–882.

Beck, H.E., Zimmermann, N.E., McVicar, T.R., Vergopolan, N., Berg, A., Wood, E.F., 2018. Present and future Köppen-Geiger climate classification maps at 1-km resolution. Sci. Data 5, 180214.

Bialik, O.M., Frank, M., Betzler, C., Zammit, R., Waldmann, N.D., 2019. Two-step closure of the Miocene Indian Ocean Gateway to the Mediterranean. Sci. Rep. 9, 8842.

Blomberg, S.P., Garland, Jr.T., Ives, A.R., 2003. Testing for phylogenetic signal in comparative data: behavioral traits are more labile. Evolution 57, 717–745.

Bolger, A.M., Lohse, M., Usadel, B., 2014. Trimmomatic: a flexible trimmer for Illumina sequence data. Bioinformatics 30, 2114–2120.

Borges, R., Machado, J.P., Gomes, C., Rocha, A.P., Antunes, A., 2019. Measuring phylogenetic signal between categorical traits and phylogenies. Bioinformatics 35, 1862–1869.

Broennimann, O., Fitzpatrick, M.C., Pearman, P.B., Petitpierre, B., Pellissier, L., Yoccoz, N.G., Thuiller, W., Fortin, M.J., Randin, C., Zimmermann, N.E., Graham, C. H., Guisan, A., 2012. Measuring ecological niche overlap from occurrence and spatial environmental data. Glob. Ecol. Biogeogr. 21, 481–497.

Brown, J.L., Hill, D.J., Dolan, A.M., Carnaval, A.C., Haywood, A.M., 2018. PaleoClim, high spatial resolution paleoclimate surfaces for global land areas. Sci. Data 5, 180254.

Burin, G., Alencar, L.R.V., Chang, J., Alfaro, M.E., Quental, T.B., 2019. How well can we estimate diversity dynamics for clades in diversity decline? Syst. Biol. 68, 47–62.

Burtman, V.S., 2000. Cenozoic crustal shortening between the Pamir and Tien Shan and a reconstruction of the Pamir-Tien Shan transition zone for the Cretaceous and Palaeogene. Tectonophysics 319, 69–92.

Burtman, V.S., Molnar, P.H., 1993. Geological and geophysical evidence for deep subduction of continental crust beneath the Pamir (Special Paper 281). The Geological Society of America, Boulder.

Capella-Gutiérrez, S., Silla-Martínez, J.M., Gabaldón, T., 2009. trimAl: a tool for automated alignment trimming in large-scale phylogenetic analyses. Bioinformatics 25, 1972–1973.

Casanovas-Vilar, I., García-Paredes, I., Alba, D.M., van den Hoek Ostende, L.W., Moyà-Solà, S., 2010. The European Far West: Miocene mammal isolation, diversity and turnover in the Iberian Peninsula. J. Biogeogr. 37, 1079–1093.

Casanovas-Vilar, I., Alba, D.M., Garcés, M., Robles, J.M., Moyà-Solà, S., 2011. Updated chronology for the Miocene hominoid radiation in Western Eurasia. Proc. Natl. Acad. Sci. USA 108, 5554–5559.

Flora of Turkey and the East Aegean Islands vol. 5, 1975, 439–450.

Djamali, M., Brewer, S., Breckle, S.W., Jackson, S.T., 2012. Climatic determinism in phytogeographic regionalization: a test from the Irano-Turanian region, SW and Central Asia. Flora 207, 237–249.

Donoghue, M.J., Sanderson, M.J., 2015. Confluence, synnovation and depauperons in plant diversification. New Phytol. 207, 260–274.

Drummond, A.J., Suchard, M.A., Xie, D., Rambaut, A., 2012. Bayesian phylogenetics with BEAUti and the BEAST 1.7. Mol. Biol. Evol. 29, 1969–1973.

Etienne, R.S., Haegeman, B., Stadler, T., Aze, T., Pearson, P.N., Purvis, A., Phillimore, A. B., 2012. Diversity-dependence brings molecular phylogenies closer to agreement with the fossil record. Proc. R. Soc. B Biol. Sci. 279, 1300–1309.

FitzJohn, R.G., 2012. Diversitree: comparative phylogenetic analyses of diversification in R. Meth. Ecol. Evol. 3, 1084–11032.

Folk, R.A., Stubbs, R.L., Mort, M.E., Cellinese, N., Allen, J.M., Soltis, P.S., Soltis, D.E., Guralnick, R.P., 2019. Rates of niche and phenotype evolution lag behind diversification in a temperate radiation. Proc. Natl. Acad. Sci. USA 116, 10874–10882.

Folk, R.A., Siniscalchi, C.M., Soltis, D.E., 2020. Angiosperms at the edge: Extremity, diversity, and phylogeny. Plant Cell Environ. 43, 2871–2893.

Fragoso-Martínez, I., Salazar, G.A., Martínez-Gordillo, M., Magallón, S., Sánchez-Reyes, L., Lemmon, E.M., Lemmon, A.R., Sazatornil, F., Mendoza, C.G., 2017. A pilot study applying the plant Anchored Hybrid Enrichment method to New World sages (*Salvia* subgenus *Calosphace*; Lamiaceae). Mol. Phylogenet. Evol. 117, 124–134.

Fu, B., Ninomiya, Y., Guo, J., 2010. Slip partitioning in the northeast Pamir-Tian Shan convergence zone. Tectonophysics 483, 344–364.

Ge, D., Zhang, Z., Xia, L., Zhang, Q., Ma, Y., Yang, Q., 2012. Did the expansion of C4 plants drive extinction and massive range contraction of micromammals? Inferences from food preference and historical biogeography of pikas. Palaeogeogr. Palaeoclimatol. Palaeoecol. 326, 160–171.

Harrison, S., Noss, R., 2017. Endemism hotspots are linked to stable climatic refugia. Ann. Bot. 119, 207–214.

Herbert, T.D., Lawrence, K.T., Tzanova, A., Peterson, L.C., Caballero-Gill, R., Kelly, C.S., 2016. Late Miocene global cooling and the rise of modern ecosystems. Nat. Geosci. 9, 843–847.

Herrando-Moraira, S., The Cardueae Radiations Group (Calleja, J.A., Carnicero-Campmany, P., Fujikawa, K., Galbany-Casals, M., Garcia-Jacas, N., Im, H.T., Kim, S. C., Liu, J.Q., López-Alvarado, J., López-Pujol, J., Mandel, J.R., Massó, S., Mehregan, I., Montes-Moreno, N., Pyak, E., Roquet, C., Sáez, L., Sennikov, A., Susanna, A., Vilatersana, R.)., 2018. Exploring data processing strategies in NGS target enrichment to disentangle radiations in the tribe Cardueae (Compositae). Mol. Phylogenet. Evol. 128, 69–87.

Herrando-Moraira, S., The Cardueae Radiations Group (Calleja, J.A., Galbany-Casals, M., Garcia-Jacas, N., Liu, J.Q., López-Alvarado, J., López-Pujol, J., Mandel, J.R., Massó, S., Montes-Moreno, N., Roquet, C., Sáez, L., Sennikov, A., Susanna, A., Vilatersana, R.)., 2019a. Nuclear and plastid DNA phylogeny of tribe Cardueae (Compositae) with Hyb-Seq data: A new subtribal classification and a temporal diversification framework. Mol. Phylogenet. Evol. 137, 313–332.

Herrando-Moraira, S., The Cardueae Radiations Group (Calleja, J.A., Chen, Y.S., Fujikawa, K., Galbany-Casals, M., Garcia-Jacas, N., Kim, S.C., Liu, J.Q., López-Alvarado, J., López-Pujol, J., Mandel, J.R., Mehregan, I., Roquet, C., Sennikov, A., Susanna, A., Vilatersana, R., Xu, L.S.)., 2020. Generic boundaries in subtribe Saussureinae (Compositae: Cardueae): Insights from Hyb-Seq data. Taxon 69, 694–714.

Herrando-Moraira, S., Nualart, N., Herrando-Moraira, A., Chung, M.Y., Chung, M.G., López-Pujol, J., 2019b. Climatic niche characteristics of native and invasive *Lilium lancifolium*. Sci. Rep. 9, 1–16.

Herrando-Moraira, S., Nualart, N., Galbany-Casals, M., Garcia-Jacas, N., Ohashi, H., Matsui, T., Susanna, A., Tang, C.Q., López-Pujol, J., 2022. Climatic Stability Index maps, a global high resolution cartography of climate stability from Pliocene to 2100. Sci. Data 9, 48.

Hillis, D.M., Bull, J.J., 1993. An empirical test of bootstrapping as a method for assessing confidence in phylogenetic analysis. Syst. Biol. 42, 182–192.

Holbourn, A.E., Kuhnt, W., Clemens, S.C., Kochhann, K.G., Jöhnck, J., Lübbers, J., Andersen, N., 2018. Late Miocene climate cooling and intensification of southeast Asian winter monsoon. Nat. Commun. 9, 1584.

Huang, Y., Clemens, S.C., Liu, W., Wang, Y., Prell, W.L., 2007. Large-scale hydrological change drove the late Miocene C4 plant expansion in the Himalayan foreland and Arabian Peninsula. Geology 35, 531–534.

Hughes, C.E., Atchison, G.W., 2015. The ubiquity of alpine plant radiations: from the Andes to the Hengduan Mountains. New Phytol. 207, 275–282.

Hughes, C.E., Nyffeler, R., Linder, P.H., 2015. Evolutionary plant radiations: where, when, why and how? New Phytol. 207, 249–253.

Hurka, H., Friesen, N., Bernhardt, K.-G., Neuffer, B., Smirnov, S.V., Shmakov, A.I., Blattner, F.R., 2019. The Eurasian steppe belt: Status quo, origin and evolutionary history. Turczaninowia 22, 5–71.

Iljin, M.M., 1962. *Jurinea* Cass., in: Shiskin, B.K., Bobrov, E.G. (Eds.), Flora of the USSR, vol. 27. Izdatel'stvo Akademii Nauk SSSR, Moscow, pp. 538–704.

Jabbour, F., Renner, S.S., 2011. *Consolida* and *Aconitella* are an annual clade of *Delphinium* (Ranunculaceae) that diversified in the Mediterranean basin and the Irano-Turanian region. Taxon 60, 1029–1040.

Jiménez-Moreno, G., Pérez-Asensio, J.N., Larrasoaña, J.C., Sierro, F.J., Garcia-Castellanos, D., Salazar, A., Salvany, J.M., Ledesma, S., Mata, M.P., Mediavilla, C., 2019. Early Pliocene climatic optimum, cooling and early glaciation deduced by terrestrial and marine environmental changes in SW Spain. Glob. Planet. Change 180, 89–99.

Johnson, M.G., Gardner, E.M., Liu, Y., Medina, R., Goffinet, B., Shaw, A.J., Zerega, N.J. C., Wickett, N.J., 2016. HybPiper: Extracting coding sequence and introns for phylogenetics from high-throughput sequencing reads using target enrichment. App. Plant Sci. 4, 1600016.

Jones, K.E., Fér, T., Schmickl, R.E., Dikow, R.B., Funk, V.A., Herrando-Moraira, S., Johnston, P.R., Kilian, N., Siniscalchi, C.M., Susanna, A., Slovák, M., Thapa, R., Watson, L.E., Mandel, J.R., 2019. An empirical assessment of a single family-wide hybrid capture locus set at multiple evolutionary timescales in Asteraceae. Appl. Plant Sci. 7, e11295.

Karl, R., Koch, M.A., 2013. A world-wide perspective on crucifer speciation and evolution: phylogenetics, biogeography and trait evolution in tribe Arabideae. Ann. Bot. 112, 983–1001.

Katoh, K., Standley, D.M., 2013. MAFFT multiple sequence alignment software version 7: improvements in performance and usability. Mol. Biol. Evol. 30, 772–780.

Köppen, W., Geiger, R., 1936. Handbuch der Klimatologie. Gebruder Borntraeger, Berlin.

Koutsodendris, A., Allstädt, F.J., Kern, O.A., Kousis, I., Schwarz, F., Vannacci, M., Woutersen, A., Appeld, E., Berke, M.A., Fang, X., Friedrich, O., Hoorn, C., Salzmann, U., Pross, J., 2019. Late Pliocene vegetation turnover on the NE Tibetan

Plateau (Central Asia) triggered by early Northern Hemisphere glaciation. Glob. Planet. Change 180, 117–125.
Kozlov, A.M., Darriba, D., Flouri, T., Morel, B., Stamatakis, A., 2019. RAxML-NG: a fast, scalable and user-friendly tool for maximum likelihood phylogenetic inference. Bioinformatics 35, 4453–4455.
Kück, P., Longo, G.C., 2014. FASconCAT-G: extensive functions for multiple sequence alignment preparations concerning phylogenetic studies. Front. Zool. 11, 81.
LaJeunesse, T.C., 2005. "Species" radiations of symbiotic dinoflagellates in the Atlantic and Indo-Pacific since the Miocene-Pliocene transition. Mol. Biol. Evol. 22, 570–581.
Lauterbach, M., Veranso-Libalah, M.C., Sukhorukov, A.P., Kadereit, G., 2019. Biogeography of the xerophytic genus *Anabasis* L. (Chenopodiaceae). Ecol. Evol. 9, 3539–3552.
Lisiecki, L.E., Raymo, M.E., 2005. A Pliocene-Pleistocene stack of 57 globally distributed benthic $\delta^{18}O$ records. Paleoceanography 20, PA1003.
López-Vinyallonga, S., Mehregan, I., Garcia-Jacas, N., Tscherneva, O., Susanna, A., Kadereit, J.W., 2009. Phylogeny and evolution of the *Arctium-Cousinia* complex (Compositae, Cardueae-Carduinae). Taxon 58, 153–171.
Louca, S., Pennell, M.W., 2020. Extant timetrees are consistent with a myriad of diversification histories. Nature 580, 502–505.
Magyari, E.K., Chapman, J.C., Gaydarska, B., Marinova, E., Deli, T., Huntley, J.P., Allen, J.R.M., Huntley, B., 2008. The 'oriental' component of the Balkan flora: evidence of presence on the Thracian Plain during the Weichselian late-glacial. J. Biogeogr. 35, 865–883.
Mahmoudi Shamsabad, M., Moharrek, F., Assadi, M., Nieto Feliner, G., 2021. Biogeographic history and diversification patterns in the Irano-Turanian genus *Acanthophyllum* s.l. (Caryophyllaceae). Plant Biosyst. 155, 425–435. https://doi.org/10.1080/11263504.2020.1756974.
Manafzadeh, S., Salvo, G., Conti, E., 2014. A tale of migrations from east to west: the Irano-Turanian floristic region as a source of Mediterranean xerophytes. J. Biogeogr. 41, 366–379.
Manafzadeh, S., Staedler, Y.M., Conti, E., 2017. Visions of the past and dreams of the future in the Orient: the Irano-Turanian region from classical botany to evolutionary studies. Biol. Rev. 92, 1365–1388.
Mandel, J.R., Barker, M.S., Bayer, R., Dikow, R.B., Gao, T.-G., Jones, K.E., Keeley, S., Kilian, N., Ma, H., Siniscalchi, C., Susanna, A., Thapa, R., Watson, L., Funk, V.A., 2017. The Compositae Tree of Life in the age of phylogenomics. Journal of Systematics and Evolution 55, 405–410.
Mandel, J.R., Dikow, R.B., Funk, V.A., Masalia, R.R., Staton, S.E., Kozik, A., Michelmore, R.W., Rieseberg, L.H., Burke, J.M., 2014. A target enrichment method for gathering phylogenetic information from hundreds of loci: an example from the Compositae. App. Plant Sci. 2, 1300085.
Matzke, N.J., 2013. BioGeoBEARS: BioGeography with Bayesian (and likelihood) evolutionary analysis in R Scripts: CRAN: The Comprehensive R Archive Network. [WWW document] URL Available from: https://cran.r-project.org/.
Mandel, J.R., Dikow, R.B., Siniscalchi, C., Funk, V.A., 2019. A fully resolved backbone phylogeny reveals numerous dispersals and explosive diversifications throughout the history of Asteraceae. Proc. Nat. Acad. Sci. USA 116, 14083–14088.
Miao, Y., Herrmann, M., Wu, F., Yan, X., Yang, S., 2012. What controlled Mid-Late Miocene long-term aridification in Central Asia?—Global cooling or Tibetan Plateau uplift: A review. Earth Sci. Rev. 112, 155–172.
Middleton, N., Thomas, D., 1997. World atlas of desertification, second ed. United Nations Environment Programme/Edward Arnold, London.
Miller, M.A., Pfeiffer, W., Schwartz, T., 2010. Creating the CIPRES Science Gateway for inference of large phylogenetic trees. Proceedings of the Gateway Computing Environments Workshop (GCE). New Orleans, LA: IEEE, 1–8.
Mittermeier, R.A., Turner, W.R., Larsen, F.W., Brooks, T.M., Gascon, C., 2011. Global biodiversity conservation: the critical role of hotspots. In: Zachos, F.E., Habel, J.C. (Eds.), Biodiversity hotspots distribution and protection of conservation priority areas. Springer, Heidelberg, pp. 3–22.
Moharrek, F., Sanmartín, I., Kazempour-Osaloo, S., Nieto Feliner, G., 2019. Morphological innovations and vast extensions of mountain habitats triggered rapid diversification within the species-rich Irano-Turanian genus *Acantholimon* (Plumbaginaceae). Front. Genet. 9, 698.
Moreau, C.S., Bell, C.D., 2013. Testing the museum versus cradle tropical biological diversity hypothesis: phylogeny, diversification, and ancestral biogeographic range evolution of the ants. Evolution 67, 2240–2257.
Morlon, H., Lewitus, E., Condamine, F.L., Manceau, M., Clavel, J., Drury, J., 2016. RPANDA: an R package for macroevolutionary analyses on phylogenetic trees. Meth. Ecol. Evol. 7, 589–597.
Morlon, H., Robin, S., Hartig, F., 2022. Studying speciation and extinction dynamics from phylogenies: addressing identifiability issues. Trends Ecol. Evol. 37, 497–506.
Mouthereau, F., 2011. Timing of uplift in the Zagros belt/Iranian plateau and accommodation of late Cenozoic Arabia-Eurasia convergence. Geol. Mag. 148, 726–738.
Nee, S., Mooers, A.O., Harvey, P.H., 1992. Tempo and mode of evolution revealed from molecular phylogenies. Proc. Natl. Acad. Sci. USA 89, 8322–8326.
Nevado, B., Atchison, G.W., Hughes, C.E., Filatov, D.A., 2016. Widespread adaptive evolution during repeated evolutionary radiations in New World lupins. Nat. Commun. 7, 12384.
Noroozi, J., Naqinezhad, A., Talebi, A., Doostmohammadi, M., Plutzar, C., Rumpf, S.B., Asgarpour, Z., Schneeweiss, G.M., 2019. Hotspots of vascular plant endemism in a global biodiversity hotspot in Southwest Asia suffer from significant conservation gaps. Biol. Conserv. 237, 299–307.
Paradis, E., Schliep, K., 2019. ape 5.0: An environment for modern phylogenetics and evolutionary analyses in R. Bioinformatics 35, 526–528.
Peterson, A.T., 2003. Predicting the geography of species' invasions via ecological niche modeling. Q. Rev. Biol. 78, 419–433.
Peterson, A., Harpke, D., Peterson, J., Harpke, A., Peruzzi, L., 2019. A pre-Miocene Irano-Turanian cradle: Origin and diversification of the species-rich monocot genus *Gagea* (Liliaceae). Ecol. Evol. 9, 5870–5890.
Potter, P.E., Szatmari, P., 2009. Global Miocene tectonics and the modern world. Earth-Sci. Rev. 96, 279–295.
Pound, M.J., Haywood, A.M., Salzmann, U., Riding, J.B., 2012. Global vegetation dynamics and latitudinal temperature gradients during the Mid to Late Miocene (15.97–5.33 Ma). Earth Sci. Rev. 112, 1–22.
R Development Core Team., 2019. R: a Language and Environment for Statistical Computing. R Foundation for Statistical Computing, Vienna, Austria http://www.R-project.org/.
Rea, D.K., Snoeckx, H., Joseph, L.H., 1998. Late Cenozoic Eolian deposition in the North Pacific: Asian drying, Tibetan uplift, and cooling of the north hemisphere. Paleoceanography 13, 215–224.
Flora Iranica vol. 139a, 1979, 180–209.
Ree, R.H., Moore, B.R., Webb, C.O., Donoghue, M.J., 2005. A likelihood framework for inferring the evolution of geographic range on phylogenetic trees. Evolution 59, 2299–2311.
Ree, R.H., Sanmartín, I., 2018. Conceptual and statistical problems with the DEC+ J model of founder-event speciation and its comparison with DEC via model selection. J. Biogeogr. 45, 741–749.
Revell, L.J., 2012. phytools: an R package for phylogenetic comparative biology (and other things). Methods Ecol. Evol. 3, 217–223.
Ribera, I., Blasco-Zumeta, J., 1998. Biogeographical links between steppe insects in the Monegros region (Aragón, NE Spain), the eastern Mediterranean, and central Asia. J. Biogeogr. 25, 969–986.
Rudov, A., Mashkour, M., Djamali, M., Akhani, H., 2020. A review of C_4 plants in Southwest Asia: an ecological, geographical and taxonomical analysis of a region with high diversity of C_4 eudicots. Front. Plant Sci. 11, 546518.
Sales, F., Hedge, I.C., 2013. Generic endemism in South-West Asia: an overview. Rostaniha 14, 22–35.
Salvo, G., Manafzadeh, S., Ghahremaninejad, F., Tojibaev, K., Zeltner, L., Conti, E., 2011. Phylogeny, morphology, and biogeography of *Haplophyllum* (Rutaceae), a species-rich genus of the Irano-Turanian floristic region. Taxon 60, 513–527.
Sayyari, E., Mirarab, S., 2016. Fast coalescent-based computation of local branch support from quartet frequencies. Mol. Biol. Evol. 33, 1654–1668.
Seehausen, O., 2015. Process and pattern in cichlid radiations - inferences for understanding unusually high rates of evolutionary diversification. New Phytologist 207, 304–312.
Shen, X., Wan, S., Colin, C., Tada, R., Shi, X., Pei, W., Tan, Y., Jiang, X., Li, A., 2018. Increased seasonality and aridity drove the C4 plant expansion in Central Asia since the Miocene-Pliocene boundary. Earth Planet. Sci. Lett. 502, 74–83.
Smith, S.A., O'Meara, B.C., 2012. treePL: divergence time estimation using penalized likelihood for large phylogenies. Bioinformatics 28, 2689–2690.
Sniderman, J.K., Woodhead, J.D., Hellstrom, J., Jordan, G.J., Drysdale, R.N., Tyler, J.J., Porch, N., 2016. Pliocene reversal of late Neogene aridification. Proc. Natl. Acad. Sci. USA 113, 1999–2004.
Stebbins, G.L., 1952. Aridity as a stimulus to plant evolution. Am. Nat. 86, 33–44.
Stroud, J.T., Losos, J.B., 2016. Ecological opportunity and adaptive radiation. Annu. Rev. Ecol. Evol. Syst. 47, 507–532.
Suc, J.P., 1984. Origin and evolution of the Mediterranean vegetation and climate in Europe. Nature 307, 429–432.
Sun, J., Gong, Z., Tian, Z., Jia, Y., Windley, B., 2015. Late Miocene stepwise aridification in the Asian interior and the interplay between tectonics and climate. Palaeogeogr. Palaeoclimatol. Palaeoecol. 421, 48–59.
Sundue, M.A., Testo, W.L., Ranker, T.A., 2015. Morphological innovation, ecological opportunity, and the radiation of a major vascular epiphyte lineage. Evolution 69, 2482–2495.
Susanna, A., Garcia-Jacas, N., 2007. In: Kadereit, J.W., Jefferey, C. (Eds.), The families and genera of vascular plants, 8. Springer, Berlin / Heidelberg, pp. 123–146.
Susanna, A., Garcia-Jacas, N., 2009. Cardueae (Carduoideae). In: Funk, V.A., Susanna, A., Stuessy, T.F., Bayer, R.J. (Eds.), Systematics, evolution, and biogeography of Compositae. IAPT, Vienna, pp. 293–313.
Susanna, A., Garcia-Jacas, N., Hidalgo, O., Vilatersana, R., Garnatje, T., 2006. The Cardueae (Compositae) revisited: insights from ITS, *trnL-trnF*, and *matK* nuclear and chloroplast DNA analysis. Ann. Missouri Bot. Gard. 93, 150–171.
Szukala, A., Korotkova, N., Gruenstaeudl, M., Sennikov, A.N., Lazkov, G.A., Litvinskaya, S.A., Gabrielian, E., Borsch, T., von Raab-Straube, E., 2019. Phylogeny of the Eurasian genus *Jurinea* (Asteraceae: Cardueae): Support for a monophyletic genus concept and a first hypothesis on overall species relationships. Taxon 68, 112–131.
Takhtajan, A., 1986. Floristic Regions of the World. University of California Press, Berkeley.
Thompson, J.A., Burbank, D.W., Li, T., Chen, J., Bookhagen, B., 2015. Late Miocene northward propagation of the northeast Pamir thrust system, northwest China. Tectonics 34, 510–534.
Uribe-Convers, S., Tank, D.C., 2015. Shifts in diversification rates linked to biogeographic movement into new areas: An example of a recent radiation in the Andes. Am. J. Bot. 102, 1854–1869.
Wen, J., Zhang, J., Nie, Z.L., Zhong, Y., Sun, H., 2014. Evolutionary diversifications of plants on the Qinghai-Tibetan Plateau. Front. Genet. 5, 4.
White, F., Léonard, J., 1991. Phytogeographic links between Africa and Southwest Asia. Flora Veg. Mundi 9, 229–246.

Wiens, J.J., Ackerly, D.D., Allen, A.P., Anacker, B.L., Buckley, L.B., Cornell, H.V., Damschen, E.I., Davies, T.J., Grytnes, J.A., Harrison, S.P., Hawkins, B.A., Holt, R.D., McCain, C.M., Stephens, P.R., 2010. Niche conservatism as an emerging principle in ecology and conservation biology. Ecol. Lett. 13, 1310–1324.

Willeit, M., Ganopolski, A., Calov, R., Robinson, A., Maslin, M., 2015. The role of CO_2 decline for the onset of Northern Hemisphere glaciation. Quat. Sci. Rev. 119, 22–34.

Winkworth, R.C., Wagstaff, S.J., Glenny, D., Lockhart, P.J., 2005. Evolution of the New Zealand mountain flora: Origins, diversification and dispersal. Organisms Div. Evol. 5, 237–247.

Wu, S.D., Lin, L., Li, H.L., Yu, S.X., Zhang, L.J., Wang, W., 2015. Evolution of Asian interior arid-zone biota: Evidence from the diversification of Asian *Zygophyllum* (Zygophyllaceae). PloS ONE 10 (9), e0138697.

Ye, X.Y., Ma, P.F., Yang, G.Q., Guo, C., Zhang, Y.X., Chen, Y.M., Guo, Z.H., Li, D.Z., 2019. Rapid diversification of alpine bamboos associated with the uplift of the Hengduan Mountains. J. Biogeogr. 46, 2678–2689.

Yoder, J.B., Clancey, E., Des Roches, S., Eastman, J.M., Gentry, L., Godsoe, W., Harmon, L.J., 2010. Ecological opportunity and the origin of adaptive radiations. J. Evol. Biol. 23, 1581–1596.

Yu, Y., Harris, A.J., Blair, C., He, X., 2015. RASP (Reconstruct Ancestral State in Phylogenies): a tool for historical biogeography. Mol. Phylogenet. Evol. 87, 46–49.

Zachos, J.C., Pagani, M., Sloan, L., Thomas, E., Billups, K., 2001. Trends, rhythms, and aberrations in global climate 65 Ma to present. Science 292, 686–693.

Zhang, Z., Han, W., Fang, X., Song, C., Li, X., 2013. Late Miocene-Pleistocene aridification of Asian inland revealed by geochemical records of lacustrine-fan delta sediments from the western Tarim Basin, NW China. Palaeogeogr. Palaeoclimatol. Palaeoecol. 377, 52–61.

Zhang, C., Rabiee, M., Sayyari, E., Mirarab, S., 2018. ASTRAL-III: polynomial time species tree reconstruction from partially resolved gene trees. BMC Bioinformatics 19, 153.

Zheng, H., Powell, C.M., Rea, D.K., Wang, J., Wang, P., 2004. Late Miocene and mid-Pliocene enhancement of the East Asian monsoon as viewed from the land and sea. Glob. Planet. Change 41, 147–155.

Zohary, M., 1981. On the flora and vegetation of the Middle East structure and evolution. In: Uerpmann, H.P., Frey, W. (Eds.), Contributions to the Environmental History of Southwest Asia, vol. 8. Reichert, Wiesbaden, pp. 1–17.

Zohary, M., 1973. Geobotanical Foundations of the Middle East (Volume I and II). Amsterdam: Gustav Fischer Verlag, and Stuttgart : Swets & Zeitlinger.